Physiochemical investigation of CO_2 accelerated concrete curing as a greenhouse gas mitigation technology

Robert A. J. Niven

Department of Civil Engineering and Applied Mechanics
McGill University, Montréal, Canada

October, 2006

A thesis submitted in partial fulfilment of the requirements of the degree for the degree of Master of Science in Environmental Engineering

Library and
Archives Canada

Published Heritage
Branch

395 Wellington Street
Ottawa ON K1A 0N4
Canada

Bibliothèque et
Archives Canada

Direction du
Patrimoine de l'édition

395, rue Wellington
Ottawa ON K1A 0N4
Canada

Your file Votre référence
ISBN: 978-0-494-28516-9
Our file Notre référence
ISBN: 978-0-494-28516-9

NOTICE:
The author has granted a non-exclusive license allowing Library and Archives Canada to reproduce, publish, archive, preserve, conserve, communicate to the public by telecommunication or on the Internet, loan, distribute and sell theses worldwide, for commercial or non-commercial purposes, in microform, paper, electronic and/or any other formats.

The author retains copyright ownership and moral rights in this thesis. Neither the thesis nor substantial extracts from it may be printed or otherwise reproduced without the author's permission.

AVIS:
L'auteur a accordé une licence non exclusive permettant à la Bibliothèque et Archives Canada de reproduire, publier, archiver, sauvegarder, conserver, transmettre au public par télécommunication ou par l'Internet, prêter, distribuer et vendre des thèses partout dans le monde, à des fins commerciales ou autres, sur support microforme, papier, électronique et/ou autres formats.

L'auteur conserve la propriété du droit d'auteur et des droits moraux qui protège cette thèse. Ni la thèse ni des extraits substantiels de celle-ci ne doivent être imprimés ou autrement reproduits sans son autorisation.

In compliance with the Canadian Privacy Act some supporting forms may have been removed from this thesis.

While these forms may be included in the document page count, their removal does not represent any loss of content from the thesis.

Conformément à la loi canadienne sur la protection de la vie privée, quelques formulaires secondaires ont été enlevés de cette thèse.

Bien que ces formulaires aient inclus dans la pagination, il n'y aura aucun contenu manquant.

Canada

Abstract

There is an emerging demand for natural and engineered CO_2 sinks to combat the effects of global warming. Carbon capture and storage (CCS) processes are expected to play a predominant role within a broad portfolio of technical innovations to mitigate greenhouse gas (GHG) emissions. A range of CCS methods will be required to provide GHG control technologies for the broad scope of industrial sectors. Within this class of technologies carbon dioxide accelerated concrete curing has the global potential to permanently and safely sequester up to 550 Mt CO_2 /yr while producing non-reinforced concrete products with improved physical properties and in less time than traditionally cured products. Previous research has exhibited shallow CO_2 penetration depth and modest CO_2 uptake in grout and concrete samples despite using severe process conditions such as high pressures, temperatures and long experimental durations. Chemical and microstructural changes during carbonation were investigated to clarify the previously unexplained limitations in CO_2 uptake and provide solutions to enhance CO_2 storage. Loss of exposed particle surface area was identified as the most significant factor limiting complete carbonation of cement grout samples. The findings were applied to design a bench scale, flow-through carbonation curing reactor that sequestered CO_2 at an average of 8.3 wt % of the cured cement with complete depth of penetration. The sequestration results were achieved with ambient temperature (20°C), 40% relative humidity, atmospheric pressure (1 atm), as-captured flue gas CO_2 partial pressure (0.20) and low flow (1 Lpm) in less than 60 minutes.

Résumé

Il y a une demande naissante de puits naturels et machinés de CO_2 pour combattre les effets de chauffage global. Selon les nombreuses innovations technologiques développées, la collecte et le stockage (CSC) du carbone sont considérés comme les processus prédominants dans l'atténuation des gaz à effet de serre. Une gamme de méthodes de CSC sera exigée afin de garantir le contrôle de ces émissions pour les secteurs industriels. Selon ces technologies, la cure accélérée du béton avec le dioxyde de carbone a le potentiel de séquestrer sans risques et de façon permanente jusqu'à 550 Mt de CO_2 tout en produisant plus rapidement les produits de béton non-renforcé possédant des propriétés physiques améliorées par rapport aux produits traditionnellement traités. La recherche précédemment a été empêchée par une faible pénétration et une absorption modeste de CO_2 dans les échantillons de coulis de ciment et béton en dépit d'employer des conditions de processus graves. Les changements chimiques et microstructuraux durant le processus ont été étudiés pour clarifier les précédents résultats obtenus et augmenter la profondeur de la pénétration ainsi que celle du stockage de CO_2. La perte de superficie exposée de particules a été identifiée comme facteur le plus significatif limitant la carbonatation complète des échantillons de coulis de ciment. Les découvertes ont été appliqués afin de concevoir un réacteur d'advection unidimensionnel à petite échelle qui carbonate pendant la cure, ayant une pénétration de CO_2 complète et permettant une stockage moyenne de CO_2 de 8.3% du poids du ciment sous température ambiante (20°C), sous pression atmosphérique avec peu de pression partielle en CO_2 (0.2) et un écoulement bas (1 Lpm), en moins de 60 minutes.

Acknowledgements

I am grateful for the technical advice and encouragement of Professor Subhasis Ghoshal throughout my research and course work. Thank you for introducing me to many aspects of environmental engineering and enabling me to offer meaningful contributions in the field of climate change.

Special thanks are needed to express my appreciation for the technical, interpretive, and administrative support from J. Bartczak, C. Chitayat, Dr. W. Cook, G. Keating, D. Kiperchuk, Dr. A. Mucci, Dr. J. Paquette, M. Przykorski, R. Sheppard, K. Zahrabi and the departmental administrative staff.

My family and friends have been a constant source of support throughout my studies. Thank you to the many new friends I have met on campus and in the McGill Outdoors Club that enriched my life with such unforgettable memories.

Table of Contents

List of Tables and Figures

1. Introduction

1.1. Global Warming

Global warming, the rising of the mean surface temperature, has been linked to rising sea levels by 0.1 - 0.2m, glacial retreat, species extinctions and habitat loss, extreme and changing weather patterns, lower agricultural yield and the spread of diseases. The last century has experienced the highest temperature gain (0.6°C) than any other century in the last 1000 years (IPCC 2001). It is now well understood that global warming is a result of anthropogenic (human-caused) activity (Bryant 1997). The most significant contributor to global warming is the rapid rise in greenhouse gas (GHG) atmospheric levels which have created a greenhouse effect (Figure 1). The four main gases, in order of greenhouse effect contribution, include water vapour (H_2O), carbon dioxide (CO_2), methane (CH_4) and ozone (O_3) (Masters 1997; IPCC 2001). However, the quantity of water vapour and ozone in the atmosphere is not significantly attributed to human activity.

Carbon dioxide (CO_2), methane (CH_4), chlorofluorocarbons (CFCs), nitrous oxide (N_2O) and fluorocarbons (CF_4) are the main anthropogenic GHGs in order of global warming effect. Since pre-industrialized times, CO_2 levels have risen 31% from 278 ppm to 365 ppm in 1998 in conjunction with rising fossil fuel consumption. This is the largest rate of change in atmospheric CO_2 levels in at least the last 20 millennia and the current CO_2 concentration is the highest in at least half a million years (IPCC 2001). According to NASA's Goddard Institute for Space Studies, 2005 was the warmest year on record since the late 1800's (Hansen, Ruedy et al. 2006). GHG levels and rising surface temperatures are expected to continue to rise over the next century by approximately 1.4

to 5.8°C. The unprecedented trend of rising temperatures has led to an era of unpredictable climate change consequences.

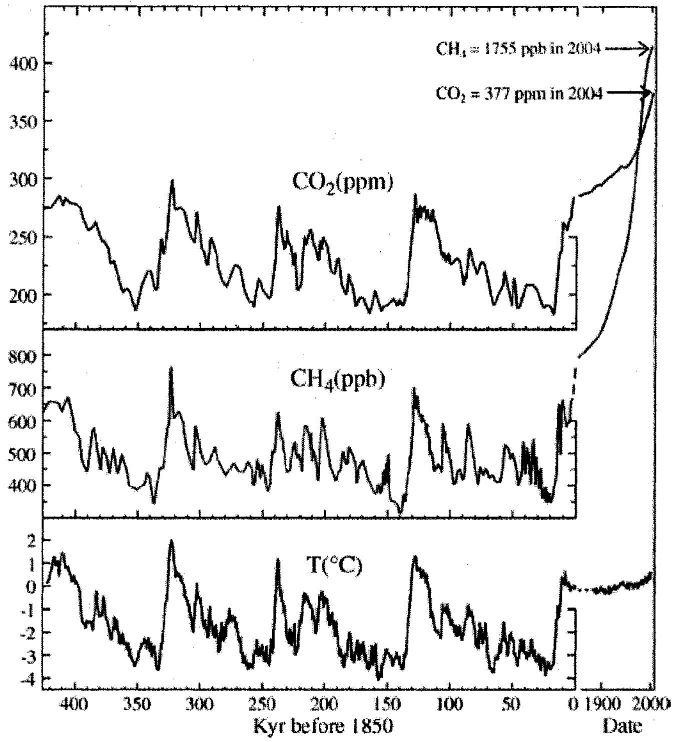

Figure 1. Historical atmospheric GHG levels and surface temperature trends (Hansen 2005).

1.1.1. The Greenhouse Effect

An energy balance exists between the earth, its atmosphere and the sun that supports life and maintains the global temperature (Bryant 1997). GHGs within the atmosphere play a critical role in maintaining the average surface temperature at 14°C; otherwise, the temperature would stabilize at -19°C. This phenomenon is considered the greenhouse effect. Energy enters the atmosphere unimpeded with a distinct wavelength (λ_{max}=0.5μm) that relates to the temperature of the radiation source – the sun. To maintain the energy balance, energy is re-emitted outwards from earth, but at a longer wavelength

(λ_{max}=101.5μm) due to its lower temperature. The atmospheric GHGs absorb more of the outgoing long wavelength energy emitted from earth than the sun's incoming short wavelength energy. A relative and time weighted energy trapping scale, the Global Warming Potential (GWP), was devised to estimate the impact of releasing a known quantity of GHG over a designated time horizon. Gases which retain more of the outgoing energy retain more heat and are assigned a higher GWP value relative to CO_2 ($GWP_{CO2} = 1$). Methane has a higher GWP ($GWP_{CH4} = 56$), but its cumulative effect is lower since less methane is released per year. In simple terms, rising GHG levels in the atmosphere retain a disproportionate amount of energy that leads to higher surface temperatures.

1.2. Response to Global Warming

1.2.1. United Nations Framework Convention on Climate Change

The greenhouse effect has been observed for decades, although it has only recently become widely accepted. The United Nations Framework Convention on Climate Change (UNFCCC) was the first international environmental treaty specifically designed to combat global warming. Since its ratification on March 21, 1994 important steps have been taken towards reaching its objective of achieving "stabilization of greenhouse gas concentrations in the atmosphere at a low enough level to prevent dangerous anthropogenic interference with the climate system" (UN 1992). Given that the treaty was voluntary and non-binding, political will was slow to develop and as a result GHG emission reductions have been modest. However, the treaty triggered a tremendous amount of research and public debate on the issue. Moreover, an overwhelming majority of the scientific community now agree that global warming is a direct result of human activity. Land use changes such as deforestation and greenhouse gas emissions, mainly CO_2 from fossil fuel combustion, were identified as the principal contributors to global warming (UN 1992). The treaty's update, the Kyoto Protocol, ratified on February 16, 2005, set legally binding emission targets and provided compliance mechanisms for all signatories (UN 1998). Annex I (developed nations) parties are bound to reduce GHG emissions by on average 5.2% below 1990 levels for the period of 2008 to 2012. If unable to reach these targets, countries may employ Kyoto mechanisms such as Joint Implementation projects (JI) with other developed countries, Clean Development Mechanism projects (CDM) with developing countries and emission credit trading (UN 1998).

1.2.2. Carbon Dioxide Capture and Storage

In order to reach these ambitious goals of reducing GHG emissions below 1990 levels, a broad spectrum of options have been suggested. Energy efficiency improvements and conservation are the preferred solutions. Other key components of any nation's GHG management plan include developing an ample, reliable and economical supply of low-carbon and renewable energy supplies (eg. wind, geothermal and solar), an effective emission management framework and technical innovations.

Carbon Capture and Storage (CCS) GHG control technologies have emerged into the forefront of the technical innovations (IPCC 2005; DOE 2006). There are three main CCS categories: ocean storage, underground geological storage and mineral carbonation. Essentially, CCS is an end-of-pipe CO_2 mitigation method that eliminates CO_2 emissions from entering into the atmosphere by storing them in various media. The processes are compatible with the existing fossil fuel infrastructure which currently provides 80% of the global energy supply and will be the primary source of energy in the foreseeable future (Holloway 2001). High purity CO_2 is captured from any large fossil fuel emission point source using one of four common technologies classes including: (1) chemical and physical solvent scrubbing, (2) adsorption, (3) cryogenic or (4) membrane systems (White, Strazisar et al. 2003; Anderson and Newell 2004). Once captured and compressed it is transported, usually by pipeline, to a suitable site where it is stored in either gaseous, super critical liquid, aqueous or solid mineral form. Depending on the CCS method CO_2 can be safely stored for decades to millennia (Herzog, Caldeira et al. 2003).

In a recent feasibility study based on 450 to 750 ppm CO_2 stabilized atmospheric concentration levels, the IPCC found that CO_2 sequestration would likely account for 15 to 55% (220-2200 Gt CO_2) of the global CO_2 mitigation effort until 2100 (2005). Many CCS processes are already technically feasible (Wilson, Johnson et al. 2003). Four commercial projects are currently in operation with combined CO_2 storage of approximately 6.5 Mt CO_2/yr, or 0.03% of the 1997 total global fossil fuel CO_2 emissions (24.2 Gt) (IPCC 2005). Many other CCS projects are in various stages of development and will be required to provide a broad portfolio of greenhouse gas management options for the wide array of industries that are forced to meet their emission control standards (Turkenburg 1997). Two planned high profile projects employing CO_2 capture and storage include the proposed FutureGen and SaskPower zero-emission coal power plants that will employ this technology to eliminate CO_2 emissions while continuing to produce power or hydrogen from coal combustion (Wilson, Tontiwachwuthikul et al. 2004; DOE 2006; SaskPower 2006). Projects that offer an economic payback like Enhanced Oil

Recovery (EOR), the injection and storage of CO_2 in depleted oil reservoirs to enhance extraction, will be deployed first (Holt 1995). Deploying the more economically favourable projects first, such as the Weyburn CO_2 sequestration - EOR project in Saskatchewan, Canada, will develop greater capacity to implement larger scale CCS projects in the future.

Underground Geological Storage

Underground geological storage has received the most attention and is used by all four of the world's commercial CCS projects. It was found that suitable storage sites exist within 300 km of most large emission point sources and provide an immense storage capacity that far exceeds 2000 Gt CO_2 (Bachu and Adams 2003; IPCC 2005). The storage costs (0.6-8.3 US$/ton CO_2) are negligible in comparison to the combined capture, separation, and compression costs (11-57 US$/ton CO_2) (Holloway 2001; IPCC 2005). Transport logistics and costs need also be considered. Dedicated pipelines have been considered to transport CO_2 from large point sources to suitable storage sites (Suncor 2006). The overall feasibility of underground geological storage improves when it is combined with value added services such as enhanced oil recovery (EOR), enhanced gas recovery (EGR) and enhanced coal bed methane recovery (ECBMR) (Anderson and Newell 2004). Moreover, long range feasibility studies must take into account advances in capture technology which will undoubtedly lower its costs.

The captured CO_2 is injected at least 800m below the surface in onshore or offshore geological formations including sedimentary basins, saline aquifers, unmineable coal beds and depleted oil and gas reservoirs that are overlaid with an impermeable cap rock

(Figure 2). The physical conditions below 800m force the gas to change phases into a supercritical fluid. As a supercritical fluid, CO_2 has higher density, yet is still more buoyant than water. The cap rock impedes its release to the surface and overtime it will become progressively better retained within the subsurface by means of various trapping mechanisms (Hendriks and Blok 1993; Bachu and Adams 2003). Ultimately, all of the CO_2 will dissolve the surrounding minerals and re-precipitate as highly stable carbonate minerals like limestone ($CaCO_3$). Carbonate minerals are the most stable CO_2 storage phase and will pose negligible environmental or health hazards (Gunter 1993).

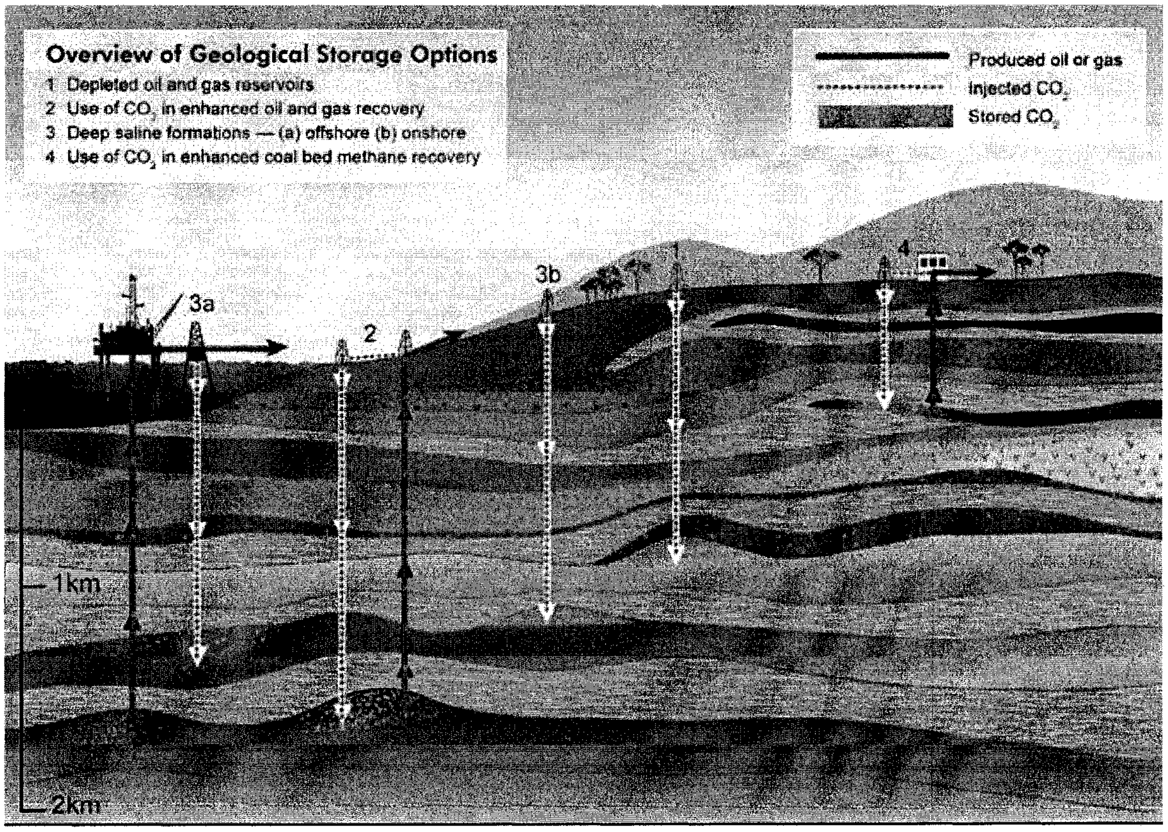

Figure 2. Schematic of Underground Geological Storage (IPCC 2005).

Careful monitoring of the injected CO_2 is carried out for the lifetime of the project. There is a risk of surface leakage creating local and global health and environmental concerns until the CO_2 forms mineral carbonates (Wilson, Johnson et al. 2003). For instance, an abrupt release of CO_2 on the surface would be fatal to nearby animal and plant life. Even slow undetected leakages would lessen the CO_2 mitigation value of CCS projects by leaving a legacy of GHG emissions for future generations. However, a great deal of expertise has already been accumulated in subsurface storage with analogous projects such as underground acid gas and natural gas storage. Drawing from these projects, safe and permanent CO_2 storage is viable.

Ocean Storage

Storage of CO_2 within oceans has also been proposed (Rau and Caldeira 1999) as an alternate method, although it is widely opposed by the public and the scientific community due to its uncertain effects on the marine ecosystem (Wilson, Johnson et al. 2003; Anderson and Newell 2004). Furthermore, it may only be applied to service point sources near the coastline. CO_2 is either dissolved 1000m below the surface or released on the ocean floor at depths below 3000m in vast supercritical pools (Figure 3). Neither method will permanently store the CO_2. Overtime CO_2 dissolves and migrates to the surface where it exchanges with the atmosphere until reaching equilibrium. Although ocean storage has a high capacity to store CO_2 there are many seemingly insurmountable challenges that preclude its implementation.

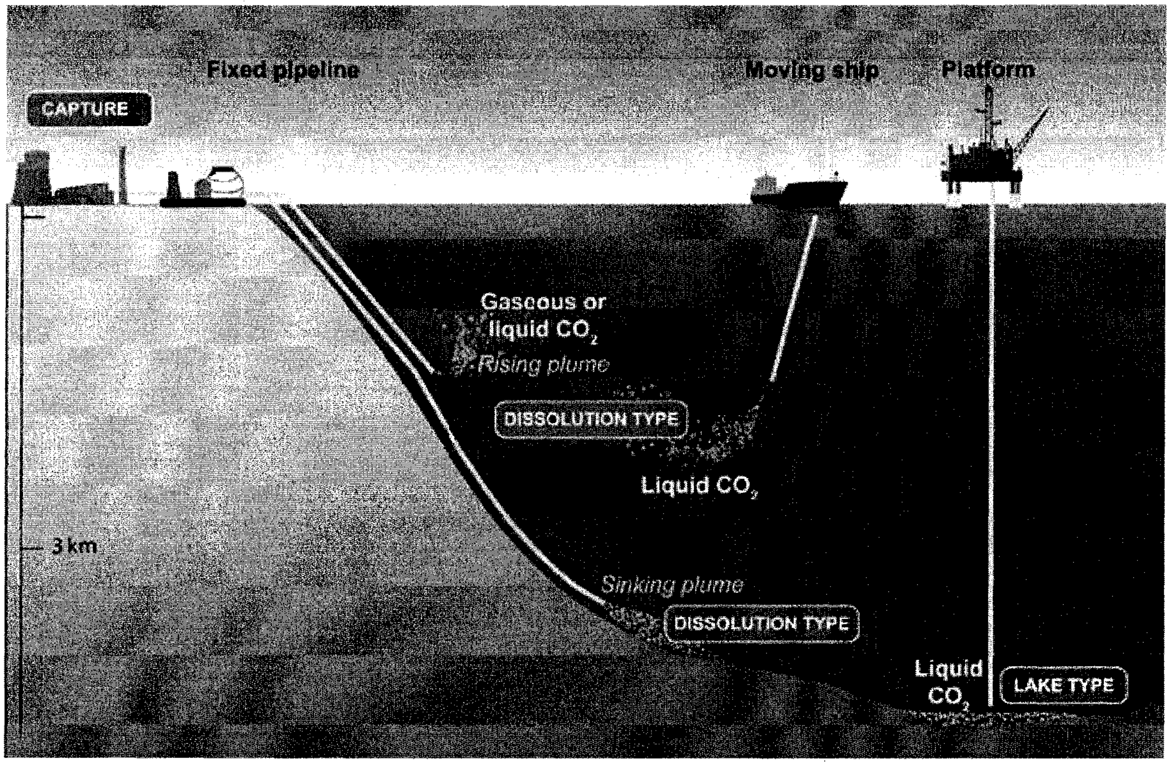

Figure 3. Schematic of Ocean Storage (IPCC 2005).

Mineral Carbonation

Mineral carbonation involves reacting CO_2 with a reactive metal oxide feedstock as seen in Figure 4. The process is closely related to lime CO_2 solid sorbent processes used to remove CO_2 from industrial flue stacks (Hughes, Lu et al. 2004). Suitable natural feedstocks include olivine, serpentine and wollastonite. Higher storage capacity per mass feedstock can be achieved by selecting materials with high aqueous reactivity, alkalinity and metal oxide (Mg or Ca) content (Lackner, Wendt et al. 1995). Unlike ocean and geological storage options, the CO_2 is entirely stored as mineral carbonates. As mineral carbonates, CO_2 is stable over millennia, environmentally benign, more dense (higher CO_2 storage per unit volume) and is immobile(Johnson, Nitao et al. 2001). There is an excess of available mineral feedstock to capture the anthropogenic release of CO_2, however mining, transporting and storing such a quantity material would have a devastating effect on the environment. Mineral carbonation is generally more expensive (50-100$/t CO_2), requires extensive storage sites for the mineral carbonate product and in some cases incurs a significant energy penalty for heat activating the material (O'Connor, Dahlin et al. 2002; IPCC 2005). The high costs, energy penalty, product disposal and mining requirements prevent mineral carbonation from becoming a viable CCS option.

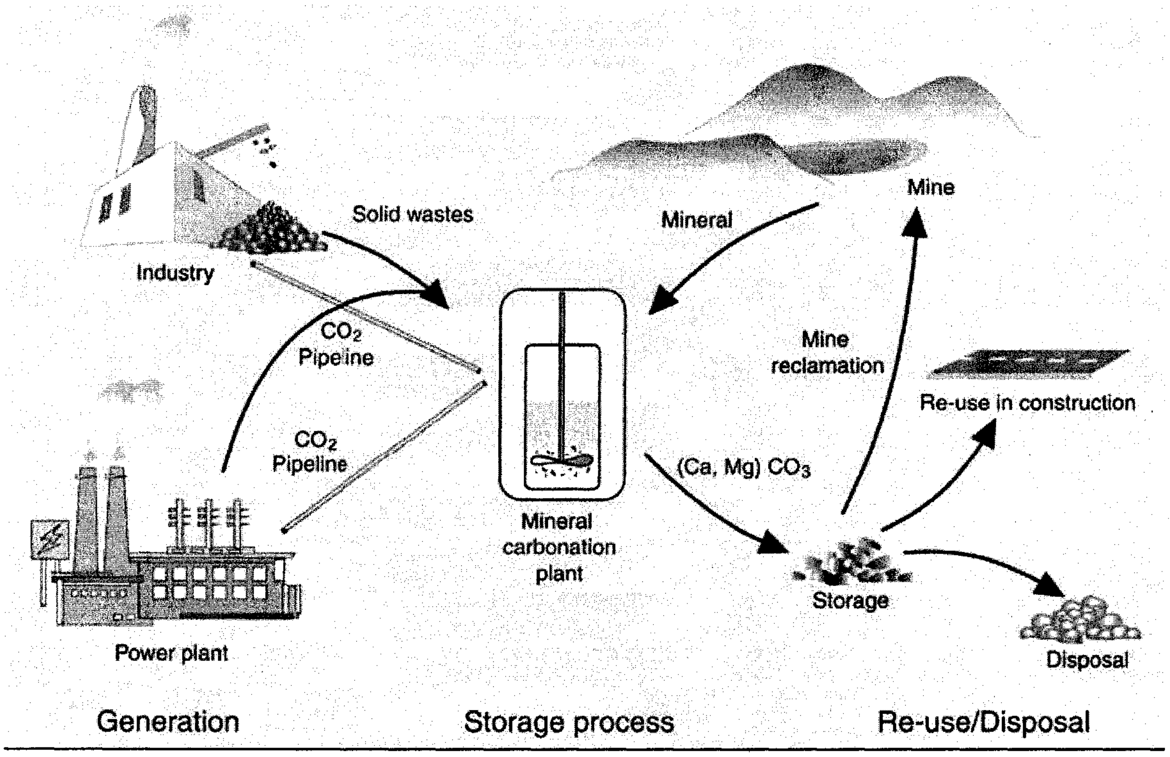

Figure 4. Schematic of Mineral Carbonation (IPCC 2005).

Carbon dioxide accelerated concrete curing is considered a mineral carbonation technique, although it is considered an economically attractive sequestration technology, because it creates value-added products through the elimination of CO_2 emissions. Furthermore, there is no carbonated waste product requiring storage and the feedstocks, in this case cement and CO_2 gas, are readily abundant and do not require energy intensive pretreatment. Moreover, carbonated concrete products are more durable, less permeable, undergo less shrinkage, and require significantly less curing time than conventionally steam cured products (Toennies 1960; Young, Berger et al. 1974; Dewaele, Reardon et al. 1991; Fernandez Bertos, Simons et al. 2004).

2. Thesis Objectives

The main objective of this work was to elucidate the concrete carbonation mechanisms and define the factors limiting the rate, extent and penetration depth of the CO_2 accelerated concrete curing process. The results identify practical mineral carbonation process enhancements and advance the knowledge of CO_2 transport and reactions in porous mineral media. The research presents detailed experimental findings of carbonating CMU surrogates with simulated flue gases found at typical large industrial point sources. Flue gas was passed through a moist, homogeneous cement grout mixture, under ambient temperature and pressure. The effects of sample moisture, carbonation time, surface area, concentration, and flow rate were investigated. Chemical and microstructural changes were monitored with two infrared gas analysis methods, backscatter scanning electron (SEM) and X-Ray diffraction (XRD) microscopy as well as X-Ray fluorescence spectroscopy.

This investigation of CO_2 accelerated concrete curing builds upon earlier findings in concrete weathering, hydration and carbonation as well as the recent advances in the fields of lime CO_2 sorbents, CO_2 injection well cement corrosion, carbon dioxide capture and storage, waste product carbonation and hazardous waste immobilization and of course CO_2 accelerated concrete curing. Presently, CO_2 accelerated concrete curing processes are operated for long durations under complicated and impractical conditions requiring high temperatures and/or CO_2 partial pressures to achieve modest CO_2 storage gains and shallow penetration. The research objectives of this project were developed with the understanding that ultimately the curing process must be viable in an industrial setting for it to be widely adopted. The research objectives of this project were to:

1. Design a model, flow-through concrete curing reactor that operates under ambient conditions and provides improved curing performance.
2. Define the factors limiting the rate, depth and extent of carbonation for the CO_2 accelerated concrete curing process.
3. Characterize the microstructural properties and classify the main constituents of the carbonated product.
4. Identify process parameters that influence the efficiency of CO_2 accelerated concrete curing.

3. Literature Review

3.1. Concrete Carbonation

Concrete, specifically cement, contains a complex mixture of minerals and is the chemically reactive component of concrete and grout during carbonation. It is an ideal mineral carbonation feedstock because it is (1) abundant and in close proximity to industrial point sources, (2) highly reactive in water under mild conditions because of its small particle size and solubility, (3) provides a value-added return on investment from improved concrete physical properties and production, (4) has high alkalinity and calcium oxide content that allows it to sequester a substantial proportion of CO_2, and lastly (5) there is no environmental or economic disposal costs (Fernandez Bertos, Simons et al. 2004).

Concrete carbonation is an exothermic and rapid process that stores CO_2 as mineral carbonates, mainly $CaCO_3$, and is facilitated by the dissolution and progressive decalcification of portlandite ($Ca(OH)_2$) and calcium silicate hydrates (C_3S, C_2S, CSH). The concrete aggregates (which are limited to sand in this study) are chemically inert, yet play a significant role in determining the initial sample permeability and porosity (Papadakis, Vayenas et al. 1989). During the transformation of cement to $CaCO_3$, the cement mineral constituents and CO_2 gas are dissolved in water as ions in the pore water. Ca^{2+} (from the cement) and CO_3^{2-} (from the CO_2 gas) ions will combine and re-precipitate as $CaCO_3$. A shortage of either Ca^{2+} or CO_3^{2-} will quench the reaction. Ion scarcity occurs when either all of the reactive feedstock has been carbonated or when ion transport limitations from microstructural adjustments are so severe that the reaction is essentially stopped (Papadakis, Vayenas et al. 1989; Reardon, James et al. 1989; Fernandez Bertos, Simons et al. 2004).

Collectively, reactions 1a to 1c outline the steps of CO_2 gas conversion to carbonate (CO_3^{2-}). The carbonate ions are produced when carbon dioxide is reacted with the grout pore water. It will first hydrate into carbonic acid (Eq. 1a) and then dissociate to form the carbonic species CO_3^{2-}, HCO_3^-, and $H_2CO_3^*$ (Eq. 1a-c). The relative abundance of the different carbonate species at equilibrium are pH dependant.

$$CO_2(g) + H_2O \rightarrow H_2CO_3^* \qquad (1a)$$

$$H_2CO_3^* \rightarrow HCO_3^- + H^+ \tag{1b}$$

$$HCO_3^- \rightarrow CO_3^{2-} + H^+ \tag{1c}$$

$$(CaO)_X \cdot SiO_2 \cdot nH_2O + 2yH^+ \rightarrow (CaO)_{x\cdot y} \cdot SiO_2 \cdot nH_2O + yCa^{2+} + yH_2O \tag{2}$$

$$Ca(OH)_2 \rightarrow Ca^{2+} + 2OH^- \tag{3}$$

$$Ca^{2+} + CO_3^{2-} \rightarrow CaCO_3 \downarrow \tag{4}$$

The calcium-bearing cement material dissolves to supply the Ca^{2+} counterions (Eq. 2 and 3). Adequate moisture is essential to enable the cement constituents to dissolve. The dissolved calcium ions rapidly react with carbonic species to form the most thermodynamically favourable and insoluble product, mainly $CaCO_3$. Once the saturation state is exceeded, $CaCO_3$ will precipitate out of solution as a solid (Eq. 4).

Water is an important by-product of concrete carbonation due to its implications on CO_2 mass transport which is explained in the following sections. The case of portlandite carbonation (Eq. 5) is illustrative of the stoichiometry and chemistry of water formation. Portlandite, is a principal hydration product of cement (see section 3.3) and is a primary source of water production in the grout sample during cabonation.

$$Ca(OH)_2 \xrightarrow{H_2O} Ca^{2+} + 2OH^- \xrightarrow{CO_2} CaCO_3(s) + H_2O \tag{5}$$

Basic concrete chemistry explains the fundamental aspects of the $CaCO_3$ formation in an ideal system without physical mass transport constraints, however, microstructural changes must also be considered to understand the CO_2 accelerated concrete process. Incomplete cement conversion to $CaCO_3$ often occurs when mass transport constraints, such as water, obstruct the mobility of ions and limit their availability. As a consequence of the limiting ion availability, concrete carbonation generally occurs in two stages; a rapid stage followed by a slow diffusion controlled stage. Specifically, the reaction kinetics are controlled by two diffusion phenomena:

(1) CO_2 gas ingress throughout the unsaturated porous network is initially caused by a rapid air advection and thin water layer diffusion process. Over the course of the reaction water is produced (Eq. 5) and saturates the pores thus eliminating the rapid air advection component of CO_2 transport. CO_2 transport through saturated pores ($D = 10^{-9}$ m^2/s) is 10 000 times slower than through unsaturated (air filled) pores (Papadakis, Vayenas et al. 1989; Van Balen 2005).

(2) The main reaction product, calcite ($CaCO_3$), is a dense (2.71 g/mol) and impermeable material with an 11.8% higher molar volume (36.9 mL) than its portlandite constituent (33.0 mL). As it is gradually deposited within the pores or on the reactive particle surfaces, it impedes CO_3^{2-} and Ca^{2+} ion mobility which inhibits continued product formation. For $CaCO_3$ formation to proceed, calcium and carbonate ions are forced to slowly diffuse through the dense $CaCO_3$ layer which has a diffusivity constant ($D = 10^{-18} - 10^{-22}$ m^2/s) that is 9 to 12 orders of magnitude smaller than water. The lower diffusion rate essentially terminates new calcite formation.

The practice of carbonating concrete products was first introduced in 1955 to improve the physical qualities of concrete products (Shideler 1955). Partial carbonation treatment is now implemented in modern CMU production plants to benefit from the greater volume stability, lower permeability, faster production and enhanced compressive strength (Toennies 1960; Freedman 1969; Young, Berger et al. 1974; Papadakis, Vayenas et al. 1989; Lange, Hills et al. 1996). The accelerated carbonation curing process also imparts rapid development of the 28-day strength rating. In laboratory test, the products reach the rating in less than 20 minutes (Shideler 1955).

Recently, it has also been recognized that concrete is also an effective CO_2 sequestration media (Fernandez Bertos, Simons et al. 2004; Harrison 2005; Logan 2006). Since carbonation treatment was already adopted within the industry for its product improvement and cost saving merits, increasing its deployment to mitigate CO_2 emissions should be welcomed by industrialists and environmentalists alike.

3.2. Concrete Weathering

Weathering, the reactions of concrete and mineral oxides with atmospheric CO_2, is the natural analogue to CO_2 accelerated concrete curing (Rau and Caldeira 1999). Evidence of weathering is apparent on the corroded surfaces of old statues and structures. Low levels of CO_2 within the atmosphere (0.035%) will form carbonic acid in the presence of moisture (Eq. 1). The same carbonation reactions (Eq. 1-4) occur in weathering. The greatest difference between the two processes is that weathering proceeds at a geological timescale due to the lower CO_2 concentration in the atmosphere. CO_2 accelerated concrete curing process conditions allow greater $CaCO_3$ formation to occur in a matter of minutes.

3.3. Concrete Hydration

In conventional concrete curing processes, hydration reactions account for the durability, strength, watertightness, abrasion resistance, volume stability and resistance to freezing and thawing and deicer salts (PCA 2006). The precipitation of the solid products, mainly polymerized calcium silicate hydrates and calcium hydroxide, from hydration reactions of cement constituents (tricalcium silicate and dicalcium silicate) provide the strength of cured concrete products. The chemistry is closely related to weathering and carbonation reactions, although carbonic acid formation (Eq. 1a) is not a principal reaction. Similarly, cement constituents will dissolve in the presence of moisture (alite shown in eq. 6). Because CO_2 levels are assumed to be relatively negligible relative to hydroxide ions (OH^-) in atmospheric conditions, the aqueous calcium ions will react with OH^- to form solid $Ca(OH)_2$ (Eq. 7). Parallel to carbonation and weathering reactions, hydration will proceed until all of the exposed cement constituents have been consumed.

$$(CaO)_3 \cdot SiO_2 \cdot nH_2O + 2H^+ \rightarrow (CaO)_2 \cdot SiO_2 \cdot nH_2O + Ca^{2+} + H_2O \tag{6}$$

$$Ca^{2+} + 2OH^- \rightarrow Ca(OH)_2 \downarrow \tag{7}$$

3.4. Conventional Concrete Curing Process

CO_2 accelerated concrete curing is an alternative concrete curing process for precast, non-reinforced, load-bearing or non-load-bearing concrete products. The precast concrete product sector consumes approximately a half of the total cement supply, equating to a global demand of 1.1 Gt/yr (van Oss 2006). Precast products are mainly comprised of concrete blocks, otherwise known within the industry as concrete masonry units (CMUs), but also include siding panels, roofing tiles, bricks, cement board, fiberboard, wall panels and concrete pipes. The standard CMU has the dimensions 20×20×40 cm and contains 12 wt % Portland cement (PCA 2006). The products are normally cured by hydration in large chambers with elevated humidity (85%) and temperature (30-50°C) for 12-24 hours (Freedman 1969). The moisture and heat is supplied by boilers situated onsite. Operating the boilers is not only a major cost of production but also imparts substantial CO_2 emissions.

3.5. Review of Applied Concrete Carbonation Research

Applied concrete carbonation research has been conducted in several domains. The principal research interest include (1) limiting reinforced concrete corrosion from CO_2 attack (Castro, Sanjuan et al. 2000; Houst and Wittmann 2002), (2) CO_2 immobilization of hazardous waste in concrete (Lange, Hills et al. 1996; Lange, Hills et al. 1996; Fernandez Bertos, Simons et al. 2004), (3) CO_2 induced decay of injection well cement (Druckenmiller, Maroto-Valer et al. 2006) and (4) CO_2 accelerated concrete curing (Reardon, James et al. 1989; Dewaele, Reardon et al. 1991; Venhuis and Reardon 2001). Investigations of limestone solid CO_2 sorbents are also of interest due to their similar application and carbonation mechanisms (Shih, Ho et al. 1999; Abanades and Alvarez 2003; Van Balen 2005). All of the research is primarily concerned with understanding the microstructural and chemical mechanisms brought on by carbonation. The carbonation conditions and material properties dictate the rate and extent of carbonation. A fundamental mechanistic understanding is required to overcome the common challenges of improving carbonation conversion rates and extent, limiting concrete corrosion in injection wells or structures and controlling the permeability of concrete to improve hazardous waste solidification.

3.5.1. Carbonation Apparatus

Selecting the appropriate carbonation apparatus is paramount in representing the actual system of interest; otherwise the results may be inapplicable in the field. For instance, to simulate the subsurface CO_2 transport in injection well concrete, it is necessary to use a high pressure and temperature reactor to simulate the supercritical conditions in the geological subsurface. For accelerated concrete curing applications, the apparatus should be transferable to an industrial process and offer the highest CO_2 uptake and penetration under the most mild process conditions. Fernandez Bertos et al. (Fernandez Bertos, Simons et al. 2004) describe the basic features of the carbonation apparatus currently employed in accelerated concrete curing research.

Generally systems may be classified as either static or dynamic. CO_2 transport in static systems is governed by diffusion. CO_2 diffusion is far slower than advection and is particularly sensitive to pore volume water saturation. For static systems, concrete specimens are placed in sealed chambers and carbonated under variable conditions. The consumed CO_2 is often replenished throughout the experiment. Typically these systems incur very shallow CO_2 penetration on the order of mere millimetres and low CO_2 uptake (12.6 wt % alite) over the course of several days or months (Young, Berger et al. 1974; Dewaele, Reardon et al. 1991). To promote penetration and uptake, high pressures have been used in static systems without much success (Reardon, James et al. 1989). The impetus was that using high pressures, more CO_2 would be introduced into the pore network before the pores were blocked with water or a calcite product layer. At 5.5 MPa CO_2 uptake was slightly enhanced (15.6 wt % cement grout), although periodic drying cycles were necessary to counteract the pore saturation that impeded CO_2 ingress. Vacuum de-airing in the presence of a desiccant was later attempted in diffusive systems to promote uptake and penetration by removing water from the pore network as it was produced, thereby maintaining unsaturated pores (Venhuis and Reardon 2001). Up to 11 mm penetration was achieved with greater CO_2 uptake than high pressure systems. Supercritical carbonation methods have also been attempted, although they offered negligible uptake or penetration benefits when compared with other high pressure static carbonation methods (Venhuis and Reardon 2001). Static systems have certain appealing features in that they employ a simple pressure chamber vessel design than can be adapted from existing industrial steam curing chambers. However, the conditions required to attain even modest CO_2 uptake and penetration (high pressure, temperature or vacuum deairation) are not practical for industrial processes.

Dynamic carbonation systems offer greater CO_2 uptake and penetration (Dewaele, Reardon et al. 1991) than static systems by transporting CO_2 into the sample using advective mass transport. CO_2 is passed through the concrete or grout specimen contained within a sealed chamber. Best results are achieved when gas short circuiting (by-passing the sample) is avoided. The apparatus design is advantageous because it effectively transports CO_2 through the sample and removes excess water vapour from the pore network. Dewaele et al. (Dewaele, Reardon et al. 1991) carbonated cement grout samples in a dynamic system where a CO_2 rich solution was forced through the sample by advection. The author's found that the high pressure dynamic process increased CO_2 uptake when compared with high pressure static systems. Unfortunately, because the samples were carbonated with a solution rather than humid CO_2 gas, the pores were saturated and the vapour removal benefits of advective transport were not tested. Dynamic systems demonstrate promising carbonation results because impractical process conditions are not required to remove the water vapour from the pores and CO_2 ingress through the sample is accelerated by advection.

The accelerated concrete carbonation curing apparatus introduced in this work employs an unsaturated dynamic (flow through) transport mechanism. In comparison to the other concrete carbonation results, the reactor achieves comparable or superior CO_2 uptake and penetration in less time using low and constant flow, temperature, pressure and CO_2 concentration. Due to the mild conditions, CO_2 uptake capacity and simple design it promises to be a viable concrete curing industrial process and CCS method.

3.6. CO_2 Mitigation Potential

The CO_2 accelerated concrete curing process can be applied to non-reinforced prefabricated concrete products. Annually, an estimated 2.2Gt of cement are produced globally (van Oss 2006). Based on UK and US cement demand surveys, 50% of cement (1.1 Gt) is consumed for CMU production (ONS 2005; van Oss 2006). At 100% efficiency CO_2 accelerated concrete curing is capable of storing approximately 50% of the weight of cement as CO_2. Applied to the global market, up to 550 Mt of CO_2 emissions are annually eligible for storage. A projected estimate of 50% carbonation efficiency would still offset 275 Mt CO_2/yr. The actual CO_2 offsets of the accelerated concrete curing process would be significantly greater because the process eliminates substantial CO_2 emissions from fuel combustion associated with the traditional steam and heat concrete curing processes.

4. Methods and Materials

4.1. Sample Preparation

The grout material was composed of Type 10 Portland cement (St. Lawrence Cement, Canada), kiln dried silica sand (Bromix) and City of Montreal tap water. The grout samples were prepared to simulate industrial concrete masonry units (CMU). One important exception was that no coarse aggregate was added in order to maintain sample homogeneity. The moist samples contained 151.9 g of cement, 607.2g of fine aggregate (silica sand) and 39.5 mL of water providing a water cement ratio (w/c) and dry density of 0.26 and 1.94 g/cm^3, respectively. Batches containing 4 samples were mixed at a time in a commercial paddle style mixer (KitchenAid). Initially the sand and cement were blended at the lowest speed setting for 30 min before adding the water in 20 mL increments over a 10 min period. The moist cement grout material was mixed for another 5 minutes to promote homogeneity. A steel mold (Figure 5A) was constructed to cast cylindrical shaped grout samples with precise sample dimensions of 12.7 cm × 3.1 cm (d × h) (Figure 5B) and even distribution of the 8 MPa applied load. Within 2 hours after casting, the samples were mounted in a PVC shell using 5-minute epoxy. Prior to carbonation the mounted samples were stored in a sealed 100% humidity chamber at room temperature for predetermined aging periods.

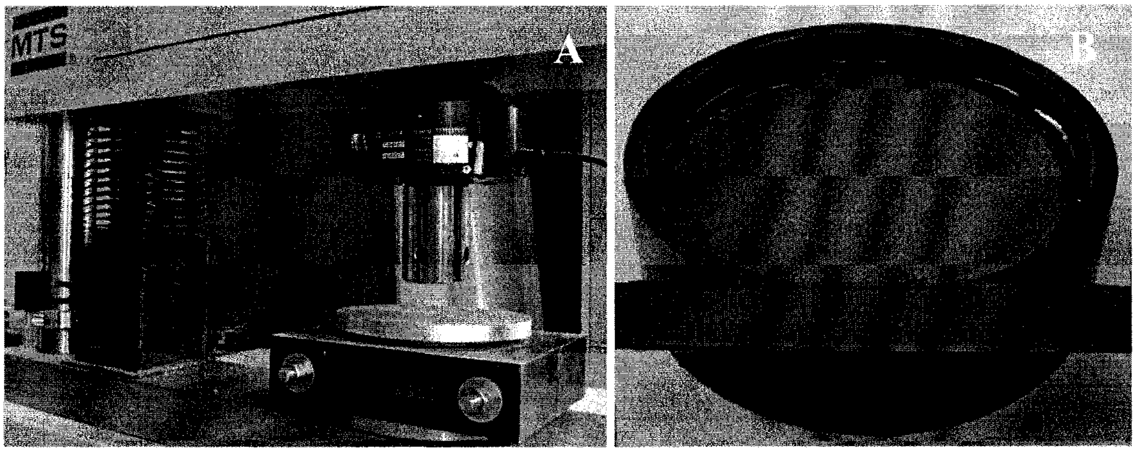

Figure 5. Sample preparation. (A) sample compaction mold (B) compacted grout sample mounted in a PVC shell.

4.2. Material Characterization

Cement was characterized for its elemental composition (Table 1) using X-Ray Fluorescence (XRF) spectroscopy with a Phillips PW2440 4k W automated spectrometer, an AFT 6000/C automated fusion preparation system and a HERZOG HTP 40 pelletizing press. The elemental composition of cement (Table 1) was required to calculate the cement phase distribution using the Bogue formula (Eq. 8) and the maximum CO_2 uptake potential according to the Steinour equation (Eq. 9). The Bogue formula estimates the relative proportion of the four primary cement powder constituents; tricalcium silicate (C_3S), dicalcium silicate (C_2S), tricalcium aluminate (C_3A), and calcium aluminate ferrites (C_4AF).

$$C_3S = 4.07CaO - 7.60SiO_2 - 6.72Al_2O_3 - 1.43Fe_2O_3 \tag{8a}$$

$$C_2S = 3.07CaO + 8.60SiO_2 + 5.07Al_2O_3 + 1.08Fe_2O_3 \tag{8b}$$

$$C_3A = 2.65Al_2O_3 - 1.69Fe_2O_3 \tag{8c}$$

$$C_4AF = 3.04Fe_2O_3 \tag{8d}$$

Table 1. Metal Oxide Characterization and Phase Distribution of Cement

Metal Oxide Composition units: wt %	CaO	63.1
	MgO	2.0
	Na_2O	0.0
	K_2O	0.0
	SO_3	3.8
	SiO_2	19.8
	Al_2O_3	5.0
	Fe_2O_3	1.7
	MnO	0.04
	Total	**95.4**
Bogue Cement Phase Distribution units: wt %	C_3S	70.5
	C_2S	3.6
	C_3A	9.6
	C_4AF	6.1
	Total	**89.8**

The particle size distributions of cement and silica sand (Table 2) were measured using a Lasentec M100 laser particle size analyzer and followed the ASTM LAS-W laser diffraction technique (Ferraris, Hackley et al. 2004) with 0.33 mm focal length, 500 rpm stirring speed, 25.6 sec readings. Cement and sand were suspended in isopropyl alcohol and deionized water, respectively.

Table 2. Particle Size Distribution of Cement and Sand

Size Categories units: μm	**Cement units: % wt**	**Sand units: % wt**
0.8-3.3	30.2	28.3
3.9-7.8	27.6	23.5
9.3-19	21.2	14.0
22-44	15.1	10.1
53-105	5.6	14.6
125-210	0.4	7.6
>250	0.0	1.9
Mean Diameter	**15.3**	**8.7**
Median Diameter	**7.4**	**40.8**
Total	**100.1**	**100.0**

4.3. Sample Carbonation

Carbonation experiments were conducted with certified high purity (± 0.1%) CO_2 gases in a nitrogen balance (Praxair Inc) in one of two reactors depending on the grout physical properties. Carbonation was conducted under a range of ambient conditions (20-40% CO_2, 1-3.4 atm, 20°C, 30-7000 min, 0.1-2 sLpm, 20-100% RH). In both reactor designs the system was operated at constant temperature, pressure, flow, CO_2 partial pressure and relative humidity. The first category, consisting of cylindrical compacted grout samples, was carbonated in the 1-D advection reactor (Figure 6A) consisting of two machined stainless steel plates with 22.9 cm × 2.5 cm (d × w) outer dimensions and a centered 12.9 cm × 1.1 cm (d × w) inset to hold the PVC sample shell in position. In the centre of each plate the gas line was connected to a threaded 0.635 cm wide female NPT connection. The abovementioned advection reactor was unsuitable for the second category of experiments involving non-compacted grout because the material was too loose to be mounted within a PVC shell. Those samples were carbonated in a custom-made 250 mL pyrex glass, three-port, continuously-stirred, gas-sparged reactor (Figure 6B). Depending on the experiment, the appropriate reactor was selected and connected to the overall apparatus. The apparatus included the analytical instrumentation (temperature/relative humidity probe, CO_2 sensor), gas control systems (pressure gauges, flow rate regulator, water trap and particulate filter) and certified gas supply (Figure 6C). Swagelok brass fittings and 0.635 cm (outer diameter) acrylic tubing were used to connect the different components of the overall apparatus. The reactors were submerged in a water bath during operation to maintain constant temperature and check for leaks.

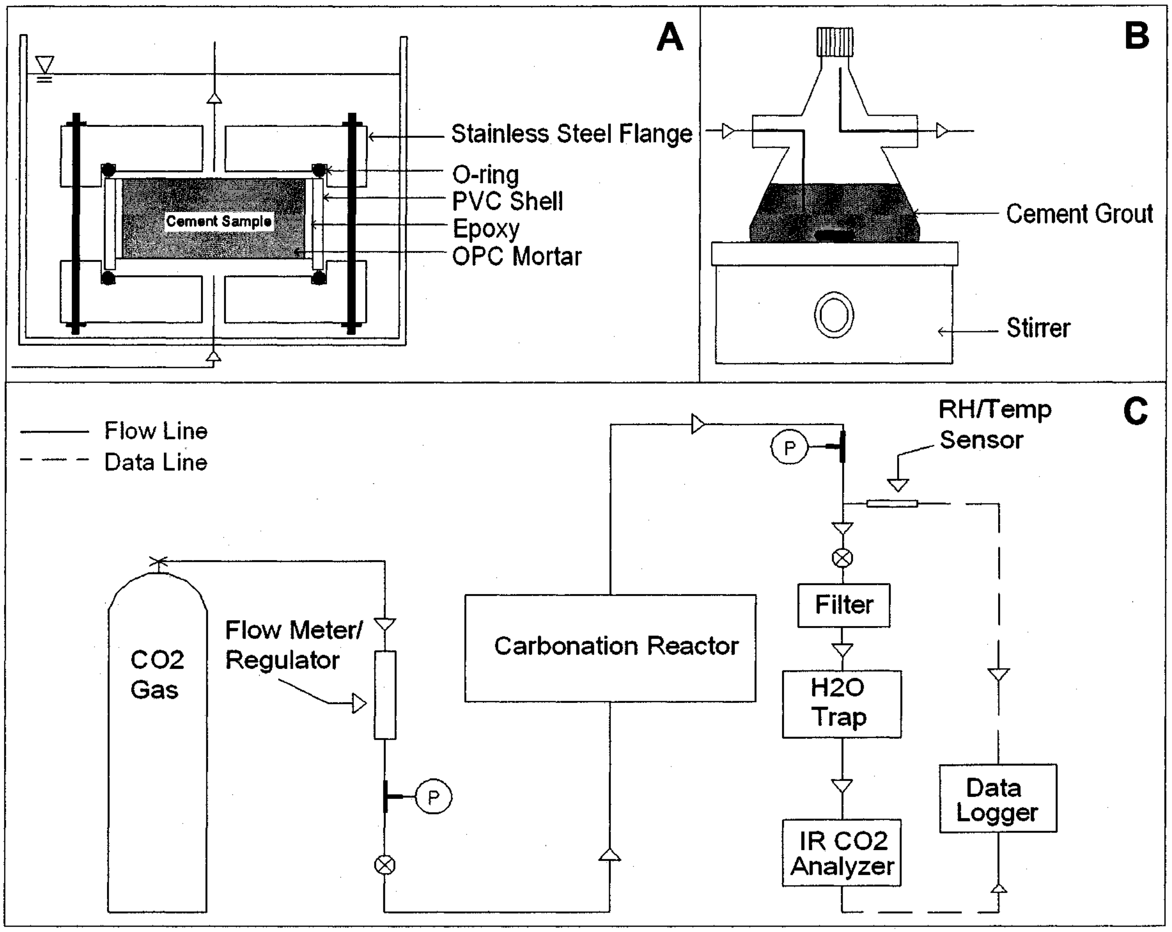

Figure 6. Carbonation apparatus (A) compacted grout reactor, (B) loose grout reactor, (C) overall carbonation apparatus setup.

4.4. Analysis Techniques

The rate and extent of CO_2 uptake were tracked using two infrared (IR) gas absorption instruments. The commonly applied and simple gravimetric assessment of mass gain during carbonation is not a suitable CO_2 uptake measurement method because unquantifiable amounts of water are produced during the reaction that must be well defined for computing the carbonation efficiency. The first IR instrument, an Eltra CS-800 combustion infrared gas analyzer, offered direct and precise measurement of the total CO_2 uptake and moisture content of solid carbonated samples after the carbonation experiment is completed. Infrared combustion analysis measures the proportional mass of carbonate species within a dried solid specimen in units of wt % CO_2. The mass of the dried sample is recorded before the sample is vaporized at high temperatures in a constant flow oxygen carrier gas. The infrared absorbance data of the effluent gas is collected and interpreted by Beer's law to measure the mass of the released CO_2 which is then compared with the initial dried mass of the sample.

In the second CO_2 measurement method, CO_2 uptake dynamics were monitored online using a Quantek model 906 NDIR CO_2 gas sensor. The instrument measures the proportional volume of CO_2 in units of vol % CO_2 contained within the effluent gas discharged from the carbonation reactors using infrared spectrographic methods explained earlier. Data from the inline CO_2 sensor and a combined relative humidity and temperature probe were collected every 5 seconds for the duration of the experiment with a multi-channel datalogger.

Following the experiment, grout samples were examined by scanning electron microscopic analysis (SEM) at the McGill materials testing services centre. A Hitachi S 4700 field emission gun SEM (FE-SEM) equipped with a Robinson backscatter detector was used to identify the major morphology and spatial distribution of the reaction products. Grout samples were electrically grounded prior to the SEM analysis by applying a 400Å Au/Pd coating. X-Ray diffraction (XRD) analysis of the carbonated material was performed to identify the morphology of the main constituents with a Phillips PW 1710 powder XRD instrument and interpreted with the 2005 ICDD diffraction pattern library.

5. Results and Discussion

5.1. Theoretical CO_2 Uptake Limit

The Steinour formula (Eq. 9) estimates the theoretical limit of CO_2 sequestration in terms of the elemental composition of the raw materials (Steinour 1959). The CO_2 uptake potential ($X_{CO_2\,Tot}$) in units of wt %, is a function of the relative mass of the specific metal oxides ($X_{CaO,\,MgO,\,SO_3,\,Na_2O,\,K_2O}$) from Table 1.

$$X_{CO_2Tot} = 0.785(X_{CaO} - 0.700X_{SO_3}) + 1.091X_{MgO} + 1.420X_{Na_2O} + 0.935X_{K_2O} \tag{9}$$

The CO_2 uptake of the water and sand (silica) was assumed to be negligible due to their low content of minerals listed in the Steinour formula. Based on the relative mass of oxides within cement (Table 1), the CO_2 uptake capacity ($X_{CO_2\,Tot}$) of cement was found to be 49.62 wt %.

5.2. Extent of CO_2 Uptake

Two calculation methods were used to calculate the carbonation efficiency (ξ) of the CO_2 accelerated concrete curing process. The carbonation efficiency calculation (ξ) (Eq. 10) quantifies the degree of carbonation by dividing the actual mass of sequestered CO_2 (M_{CO_2}) in Kg by the maximum potential mass of sequestered CO_2 ($M_{CO_2\,Tot}$) in Kg. The maximum carbonation efficiency (100%) of a completely carbonated sample would contain approximately 50% of the weight of cement as sequestered CO_2. On average a carbonation efficiency of 16.7 ± 2.1%, which is equivalent to 8.3 wt % of cement as CO_2, was attained for compacted grout samples using standard carbonating conditions (1 sLpm, 20% CO_2, w/c = 0.26, 40% RH, 20°C, 1 atm, 60 min) in the 1-D advection reactor. The first and main method used to report the carbonation efficiency applied the combustion infrared gas analysis data to calculate the total CO_2 uptake of fully carbonated samples. The second method used the inline infrared CO_2 gas analysis data to track the CO_2 uptake in 5 second intervals and to also calculate the carbonation efficiency of the fully carbonated sample. Both methods compared well for the wide range of experimental conditions tested (0.1-2 Lpm, 20- 40% CO_2, 20-100% RH, 20°C, 1-3.4 atm, 30-7000min).

5.2.1. Combustion IR Carbonation Efficiency Calculation

The calculation is based on data obtained from the combustion infrared (IR) data, mass measurements of the starting materials and the XRF chemical composition results for cement. Corrections were made to normalize the carbonation efficiency for the mass of cement contained within the product and to account for the pre-existing carbonate content of unreacted cement (Eq. 11). (M_P) is the mass of the dry carbonated grout sample in Kg, (X_{CO_2}) is the proportion of CO_2 within the dry carbonated grout sample in wt % CO_2, ($X_{CO_2}^{o}$) is the existing proportion of CO_2 content within the sample prior to carbonation (7.1 wt %), (M_C) is the mass of cement powder initially added to the sample in Kg and ($X_{CO_2\,Tot}$) is the proportional CO_2 uptake capacity of cement calculated by the Steinour equation (Eq. 9) in wt % CO_2.

$$\xi = \frac{M_{CO_2}}{M_{CO_2 Tot}} \qquad (10)$$

$$\xi = \frac{(X_{CO_2} - X_{CO_2}^{\circ}) * M_P}{X_{CO_2 Tot} * M_C} \qquad (11)$$

A final correction was made to replace the mass of the dry carbonated product (M_P) with more quantifiable masses of the fine aggregate (sand) (M_F) and cement (M_C). Equation 12 is given by understanding that the numerators of equations 10 and 11 are equivalent.

$$M_{CO_2} = (X_{CO_2} - X_{CO_2}{}^{\circ}) * M_P \tag{12}$$

The dry mass of the carbonated product (M_P) is equal to the sum of the masses of cement, sand and sequestered CO_2 (M_{CO_2}) as seen in equation 13. The mass of the dry product (M_P) is eliminated in equation 12 by substituting equation 13 into 12 and solving for M_{CO_2} as seen in equation 14. Lastly, substitute equation 14 into the numerator of equation 11 to receive the final simplified carbonation efficiency (Eq. 15). The simplified equation eliminates the necessity to estimate changes in mass of the final product from water accumulation and handling material losses. M_F and M_C were measured during the sample preparation while X_{CO_2} and $X_{CO_2}{}^{o}$ were obtained from combustion infrared analysis.

$$M_P = M_C + M_F + M_{CO_2} \tag{13}$$

$$M_{CO_2} = (\frac{M_F}{M_C} + 1) * Mc * \frac{X_{CO_2} - X_{CO_2}{}^{\circ}}{1 - (X_{CO_2} - X_{CO_2}{}^{\circ})} \tag{14}$$

$$\xi = \frac{(\frac{M_F}{M_C} + 1)}{X_{CO_2 Tot}} * \frac{X_{CO_2} - X_{CO_2}{}^{\circ}}{1 - (X_{CO_2} - X_{CO_2}{}^{\circ})} \tag{15}$$

5.2.2. Inline IR Carbonation Efficiency Calculation

The real time effluent CO_2 data provided valuable insights into the extent and dynamics of the carbonation reaction. The second carbonation efficiency calculation method was based on three variables; the CO_2 concentration data from the inline NDIR analysis of the reactor effluent gas (C_{CO_2}'), mass of cement in the sample (M_C) and time (t). Certified CO_2 mixtures in a nitrogen balance were used to carbonate the samples with constant inlet concentration ($C_{CO_2}^{o}$) as shown in plot C of a typical carbonation plot (Figure 7). The concentration of the effluent gas (C_{CO_2}') was measured and recorded every five seconds ($\Delta t = 5s$) after it passed through and reacted with a compacted cement grout sample. The effluent CO_2 concentration is shown in plot D of Figure 7. Relative humidity (plot A) and temperature (plot B) were also recorded in 5 second intervals to confirm that isothermal and constant humidity conditions were maintained. The mass of sequestered CO_2 (M_{CO_2}) for each time interval (Δt) was calculated using equation 16. Equation 16 is a function of the inlet gas CO_2 concentration ($C_{CO_2}^{o}$) in vol % CO_2, the effluent CO_2 gas concentration in vol % CO_2, the constant gas flow (Q) in L s^{-1}, time (t) in s and the CO_2 gas density in kg L^{-1}. The sum of all intervals for any time period provided the cumulative CO_2 mass gain. The second carbonation efficiency (ξ) calculation (Eq. 17) was a function of the cumulative CO_2 mass gain (M_{CO_2}) in Kg, the CO_2 uptake potential of cement ($X_{CO_2\,Tot}$) in wt % CO_2 and the dry mass of cement within the sample (M_C) in Kg.

$$M_{CO_2} = (C_{CO_2}^{\circ} - C_{CO_2}') * Q * \Delta t * \rho_{CO_2} \tag{16}$$

$$\xi = \frac{M_{CO_2}}{X_{CO_2 Tot} * M_C} \tag{17}$$

5.3. CO_2 Uptake Dynamics

Two distinct stages in the CO_2 uptake patterns were observed during the carbonation of compacted and non compacted cement grout as displayed in a typical plot under standard conditions in Figure 7. It can be seen that the vast majority of the CO_2 uptake occurs during the initial stage I and that there is no activation period preceding the rapid uptake. During the course of this approximately 30 minute period, all of the CO_2 was removed from the gas stream, demonstrating the fast kinetics and sequestration potential of cement products. The cumulative mass gain from CO_2 storage (plot E) exemplifies the high proportion of sequestration occurring within this short period. Stage I carbonation was observed to gradually decline and eventually impart negligible CO_2 uptake as seen in stage II. Typically the carbonation reaction ran to completion within one hour without reaching complete conversion. Long term carbonation experiments (7 days) did not offer any additional CO_2 uptake or loss.

The CO_2 uptake curve (plot D) contains a significant source of error from entrapped air (low CO_2 content) within the apparatus before carbonation was started. The existing volume of air diluted the CO_2 effluent thus negatively skewing the actual CO_2 readings and exaggerating the CO_2 uptake calculations. This effect would be relevant only for approximately the first 3 minutes of the carbonation process for a flow-rate of 1L/min. Effort was made to limit this source of error by minimizing the internal volume of the apparatus. Due to this effect, the inline CO_2 data was not used to calculate the reported carbonation efficiency values. Rather the combustion infrared calculation method was used which is not affected by the same source of error.

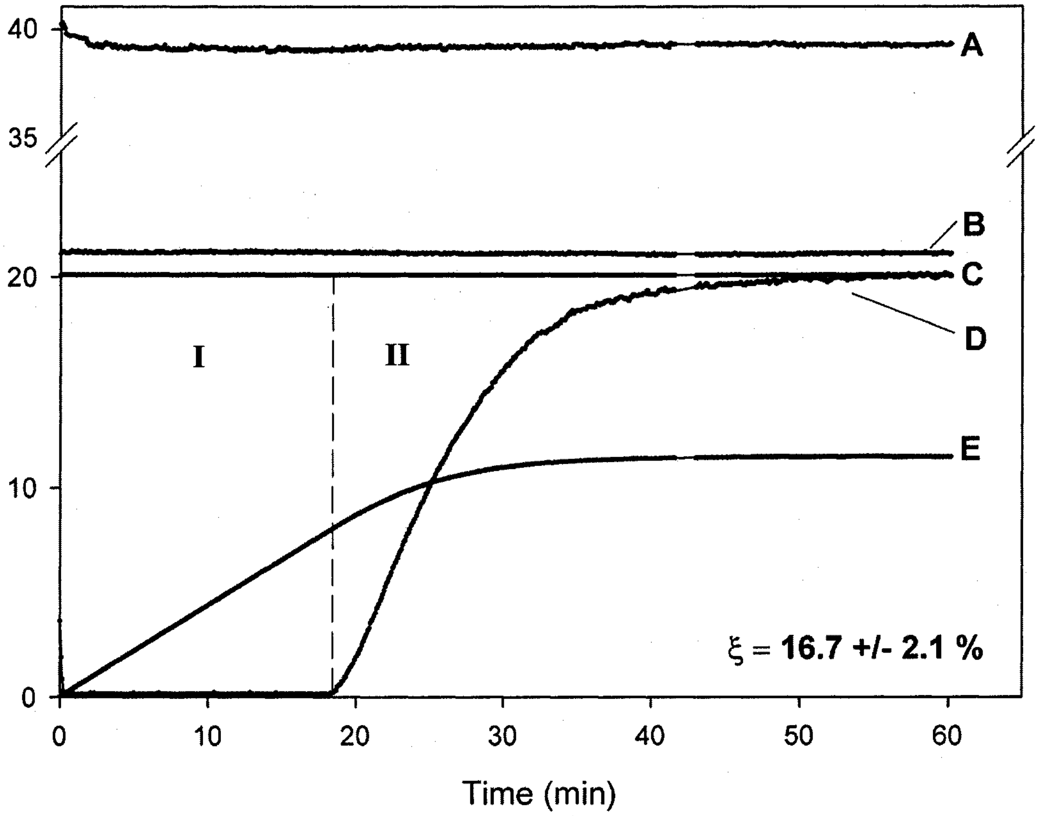

Figure 7. Carbonation plot of compacted cement grout. (A) RH (%), (B) temperature (°C), (C) inlet CO_2 concentration (%) , (D) outlet CO_2 concentration (%), (E) cumulative CO_2 mass gain (g). The error bar denotes the standard deviation ($\sigma = 1$) of replicate samples.

CO_2 accelerated concrete curing involves many concurrent physiochemical changes throughout the duration of the reaction. There is no clear consensus in the literature on the governing factors that control the rate of reaction and limit the extent of carbonation. Relative humidity (Papadakis, Vayenas et al. 1989), CO_2 hydration (Fernandez Bertos, Simons et al. 2004), portlandite dissolution (Shih, Ho et al. 1999; Van Balen 2005), $CaCO_3$ deposition (Bhatia and Perlmutter 1983; Dewaele, Reardon et al. 1991; Abanades and Alvarez 2003; Huijgen, Witkamp et al. 2005) and moisture content (Young, Berger et al. 1974; Reardon, James et al. 1989; Venhuis and Reardon 2001) have been proposed as the main factors controlling the reaction in various lime and concrete carbonation experiments. The CO_2 accelerated concrete curing mechanism was studied to clarify the governing factors under a range of ambient conditions (20-40% CO_2, 1-3.4 atm, 20°C, 30-7000 min, 0.1-2 sLpm, 20-100% RH) in a flow through carbonation reactor. As discussed earlier, stage I carbonation kinetics are extremely rapid and are followed by declining CO_2 uptake seen in stage II. Stage I and II reactions are only differentiated for the purpose of discussion and in reality are closely interrelated. Since the CO_2 uptake in stage II is relatively low, the overall process efficiency is mainly controlled by stage I. An investigation of the stage I physiochemical changes was applied to propose carbonation curing guidelines for improved efficiency and dynamics. It was found that sample hydration time (aging) and CO_2 supply rate were the main factors controlling the carbonation dynamics in stage I.

5.3.1. Effects of Hydration Time

Unique carbonation dynamics were observed for samples that were hydrated (aged) prior to carbonation. In the context of this study, aging or hydration time refers to the elapsed time from when moisture is first added to the dry grout material until the start of the sample carbonation. During this period, concrete hydration is the dominant reaction (Eq. 6-7). For aging periods longer than approximately 20 hours, the carbonation plot displayed slower uptake within stage I as shown in Figure 8, plot A. Hydration reactions and accompanying microstructural changes caused by aging were found to be the cause of the anomaly that limited CO_2 uptake in stage I.

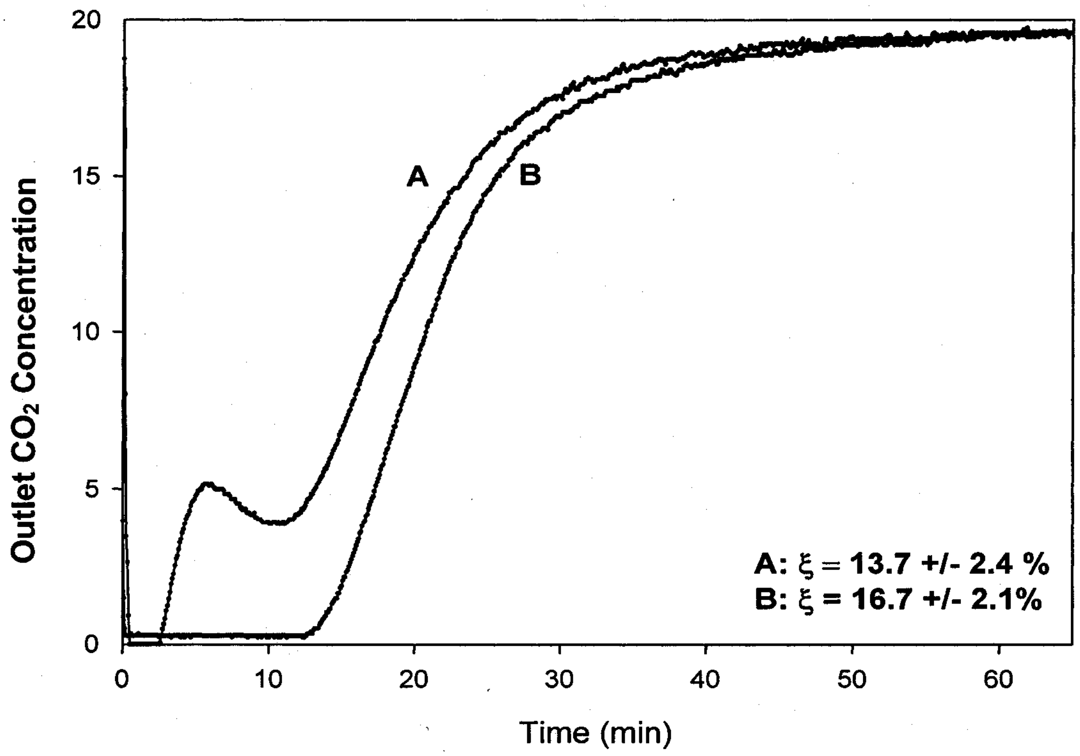

Figure 8. Carbonation plots of aged grouts. (A) aged and (B) unaged. Error bars denote the standard deviation ($\sigma = 1$) of replicate samples.

Similar to carbonation reactions, hydration reactions spontaneously occur in moist grout samples that deposit a low permeability product layer across the unreacted material which impedes subsequent reactions. Both carbonation and hydration reactions dissolve the cement constituents, consisting mostly of C_3S with gradually increasing proportions C_2S and CSH as C_3S is decalcified (Eq. 2). The Ca^{2+} ions will form the most thermodynamically stable compound with the available counterions. Under exposure to atmospheric CO_2 levels, the cement grout pore water is highly basic (pH = 12.5) and alkaline, which amounts to a scarce supply of CO_3^{2-} ions in comparison to the amount of available OH^- ions (Glass, Reddy et al. 2000; Fernandez Bertos, Simons et al. 2004). Due to the relative lack of carbonate ions, the main reaction product is $Ca(OH)_2$, which precipitates out of solution as portlandite once the saturation state is exceeded (Eq. 7).

Portlandite will form in the absence of CO_2, but will readily dissolve and reprecipitate as $CaCO_3$ once moist CO_2 is introduced.

Portlandite precipitates on the particle surfaces and within the pore network as shown in the SEM micrograph of hydrated cement grout (Figure 9B). The distinctive infilling of aged samples with hydration reaction products is clearly observed when the SEM micrographs of aged and unaged samples are compared in Figures 9A and 9B, respectively. The massive infilling is dominated with densely packed amorphous CSH (Figure 9C) embedded with sporadic clusters of mixed crystal structures (Figure 9D) that have been characterized and found to contain portlandite, gypsum and traces of aragonite. Aragonite is the kinetically favoured yet metastable $CaCO_3$ polymorph.

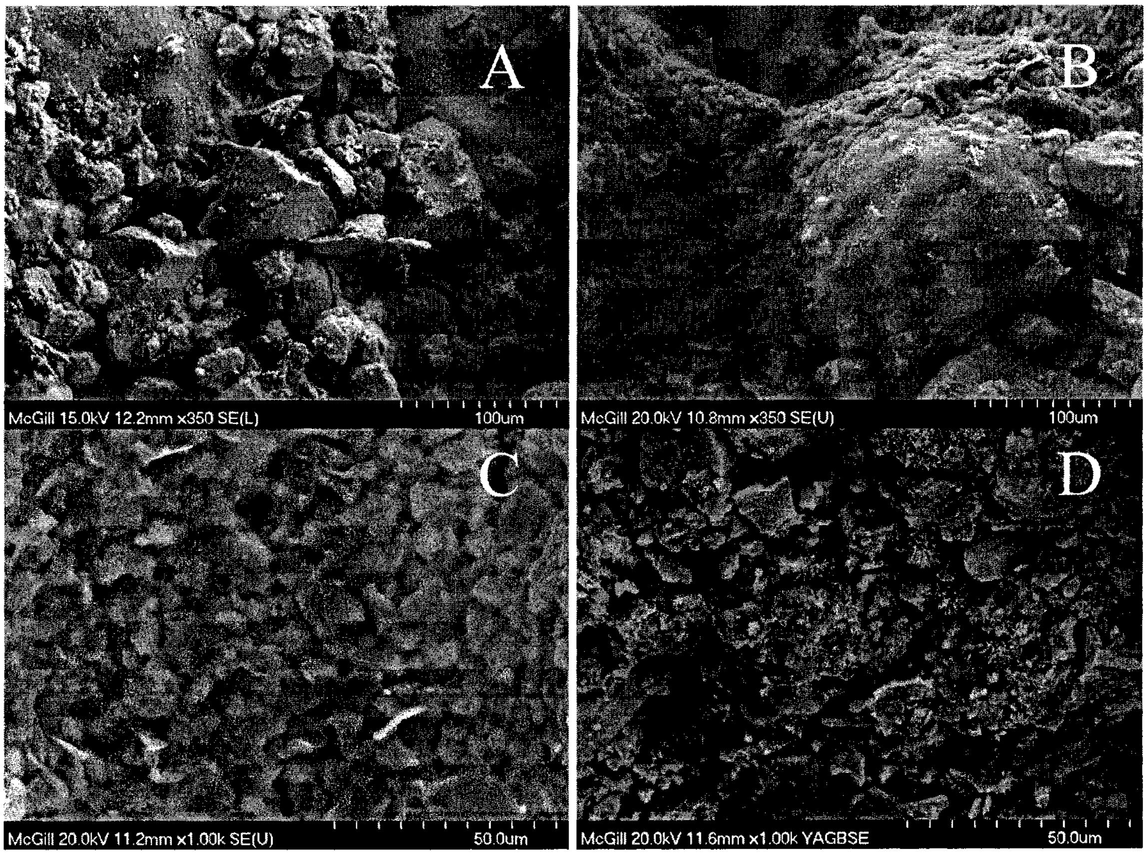

Figure 9. SEM micrograph of grout samples. (A) unaged grout, (B) aged grout, (C) amorphous CSH, (D) embedded crystal structures.

The early peak witnessed in the carbonation profile of the aged sample (Figure 8A) is likely linked to the hydration product infilling seen in Figure 9B. The deposited hydration products impede the CO_2 ingress into the entire pore network and carbonation of coated unreacted cement material. In effect the hydration product layer must be dissolved by carbonic acid prior to carbonating the unreacted material below. However, as also found by Van Balen (Van Balen 2005), the rate of portlandite dissolution is much slower than carbonation. The carbonation uptake resumes once the hydration product layer begins to dissolve and when the underlying unreacted cement particles become exposed, as shown by the increasing uptake rate in the latter half of stage I (Figure 8A). The extent of carbonation is also lower in aged samples. The lower carbonation efficiency is likely due to hydration product pore blockages and particle surface coatings that are only partially dissolved before being covered with an insoluble $CaCO_3$ product layer. The segregated material is then unavailable for the ensuing carbonation.

5.3.2. Stage I CO_2 Supply Rate Considerations

Stage I occurred for approximately 30 minutes in standard carbonation conditions of unaged samples. The duration of the first stage was related to the time required to coat the unreacted surface areas. In Figure 10, it was observed that the duration of stage I was nearly linearly related to the amount of CO_2 injected into the system, as discussed later. In stage I, all of the injected CO_2 is captured and stored, therefore the amount of CO_2 added is directly related to the quantity of product formed. Since the maximum product layer thickness is held at 0.1 μm (Abanades and Alvarez 2003), the amount of injected CO_2 is also related to the surface area covered. $CaCO_3$ is the major carbonate product and deposits within the pore network and upon the particle surface areas. It can be considered that the unreacted grout material has limited surface area capable of $CaCO_3$ deposition (Abanades and Alvarez 2003; Van Balen 2005). Once this surface area is covered with an impermeable $CaCO_3$ product layer, mass transport becomes severely limited by diffusion across the $CaCO_3$ boundary and further $CaCO_3$ production is nearly halted as witnessed in stage II. After stage II, $CaCO_3$ formation will continue at the much slower product layer diffusion controlled reaction rate; however, it is negligible in terms of an industrial process timescale.

In a dynamic flow through reactor design for the compacted grout samples and prior to complete product layer coverage, CO_2 is rapidly distributed throughout the unsaturated pore network by advection. In pressure chamber carbonation apparatus (no advective flow of CO_2 through the sample), which have been commonly employed for accelerated concrete curing studies (Reardon, James et al. 1989; Venhuis and Reardon 2001), CO_2 transport is controlled by a slower diffusion process of CO_2 into the interior of grout samples. The CO_2 dissolves in the bulk water layer, covering the particle and pore surface areas. Carbonic acid is formed (Eq. 1a) and dissociates to reach the pH-controlled distribution of carbonic species (Eq. 1a-c). Carbonate and calcium ions quickly exchange across the water boundary layer (diffusion coefficients, $D \sim 10^{-9}$ m^2/s) and form $CaCO_3$ (Papadakis, Vayenas et al. 1989; Shih, Ho et al. 1999). The rate is rapid ($k = 3.99\times10^{-4} - 2.84\times10^{-3}$ s^{-1}) and is thus not the rate determining factor (Van Balen 2005). In comparison, the rate of ion diffusivity across the $CaCO_3$ product layer is 9 to 12 orders of magnitude slower ($D \sim 10^{-18} - 10^{-22}$ m^2/s) than across a water boundary (Bhatia and Perlmutter 1983).

The duration of stage I is directly related to the amount of CO_2 injected into the system which defines the extent of product layer coverage. The CO_2 concentration and flow rates were adjusted to control the CO_2 injection rate. The grout carbonation profile under higher CO_2 concentration (plot A) and variable flow rates (plot B and D) are shown in Figure 10. Adjustments in carbonation parameters are compared with the standard carbonation curve (plot C). Unless specified, all carbonation conditions were kept constant for each sample type.

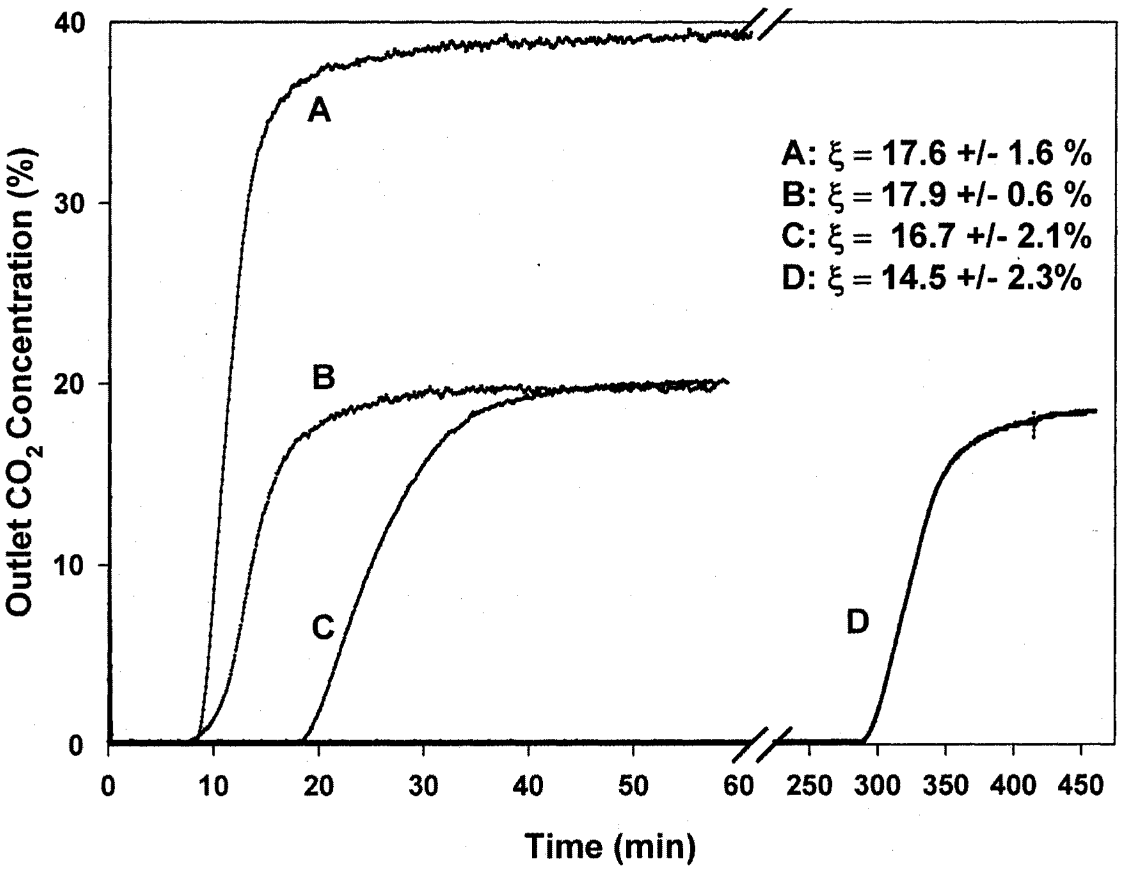

Figure 10. Carbonation plots of compacted grout under variable CO_2 concentration and flow. (A) 40% CO_2, 1 Lpm (B) 20% CO_2, 2 Lpm, (C) 20% CO_2, 1 Lpm (D) 20% CO_2, 0.1 Lpm. The carbonation efficiency error denotes the standard deviation ($\sigma = 1$) of replicate samples.

It was found that by doubling the amount of CO_2 added to the system per unit time - either by doubling the CO_2 concentration (plot A) or doubling the flow rate (plot B) - the stage I duration of the control group (18 min) was reduced by a factor of 2, suggesting a linear relationship between the CO_2 rate and the duration of stage I. For both cases stage I ended simultaneously at 9 minutes and the difference between the carbonation efficiencies (17.6 and 17.9%) was not statistically significant according to the T-test analysis with $\alpha = 0.05$ and df = 4. The higher uptake efficiency is likely a result of forcing more CO_2 into remote pores before they were blocked by $CaCO_3$ plugs. The CO_2 supply rate dependency was less pronounced for low flow circumstances. The CO_2 concentration was maintained at 20%, but the flow rate was reduced by a factor of 10. In this case, stage I terminated approximately 100 min later than expected (290 min), but yielded lower carbonation efficiency (14.5%) than the control group (16.7%) or the enhanced CO_2 supply groups (17.6 and 17.9%).

Without any attempt to promote CO_2 uptake in stage II, the kinetics and overall uptake can be easily enhanced by increasing the CO_2 supply rate and minimizing the aging time of samples carbonated in a flow through carbonation curing reactor. Raising the concentration of CO_2 would be costly, however, increasing the flow rate is far more practical since abundant CO_2 flue gases may be employed. Minimizing aging time poses no perceived disadvantages since aging time lengthens the industrial production cycle, thereby raising costs, and is not required for product strength development in accelerated concrete curing. Concrete curing offers equivalent strength development in less than 20 minutes with CO_2 accelerated concrete curing than what is normally achieved in 28 days using conventional hydration curing methods (Young, Berger et al. 1974).

5.4. CO_2 Uptake Limitations

It has been shown that the onset of stage II occurs when the available particle and pore surface area is coated with an impermeable $CaCO_3$ product layer that essentially halts ion diffusion. The process is analogous to portlandite deposition in that the precipitates will deposit within pores (Figure 11B) and on particle surfaces (Figure 11C). The two deposition processes are distinguished by the relative solubility of the products. In the case of portlandite, it is more soluble than calcite and will dissolve upon carbonation. As a soluble layer it will only impose a temporary ion transport limitation until it is dissolved. The carbonation product layer, mainly $CaCO_3$, is insoluble and will impose permanent ion diffusion limitations. The extent of deposition in carbonated samples can be appreciated by comparing the SEM micrographs of carbonated and non-carbonated samples in Figure 11. Non carbonated samples (Figure 11A) exhibit cleaner surfaces and negligible pore infilling.

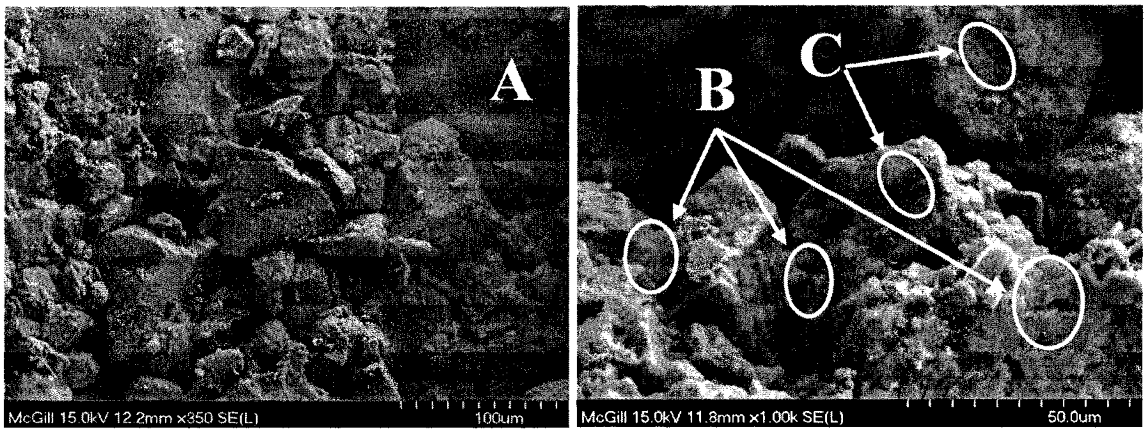

Figure 11. SEM micrographs of grout samples. (A) non-carbonated, (B) interstitial $CaCO_3$ infilling, (C) surface $CaCO_3$ deposition.

5.4.1. Spatial Distribution of Carbonation Products

As observed in Figure 11 B and C, the $CaCO_3$ product layer may deposit on individual particle surfaces or on the interstitial porous network walls. Interstitial infilling will cause pore diameter narrowing, increased tortuosity, and eventual blockage of narrow pores. The blockages may impede CO_2 access into entire unreacted zones within the pore network causing heterogeneous mineral carbonate formation. The carbonation efficiency heterogeneity is reflected in the error bars of solid grout samples as seen in Figure 12. As expected, the heightened heterogeneity from pore blockages is less pronounced (smaller error bar) near the inlet surfaces (Figure 12B) since CO_2 access is not impeded. The second category of product layer coverage, individual particle surface deposition, will also limit CO_2 uptake, although it does not cause localised moisture and carbonation heterogeneity.

Shih et al. (Shih, Ho et al. 1999) explained that the relative proportion of $CaCO_3$ deposits between the two location types is governed by the moisture content. The effect for both phenomena is the same, whereby the rate of carbonation becomes controlled by ion diffusion across the product layer once either surface area type (pore or particle) is covered.

The extent of carbonation across the depth of the sample is also expressed in Figure 12. As seen in the carbonation efficiencies at different depths of the treated samples, nearly uniform calcite distribution across the sample depth was achieved using very mild conditions (1 sLpm, 20% CO_2, 40% RH, 20°C, 1 atm, 60 min) with simulated as-captured flue gas. The findings contrast with the typical observations of concrete carbonation experiments performed in static reactor types, which incur shallow penetration depths (< 5 mm) using more severe process conditions (Young, Berger et al. 1974; Dewaele, Reardon et al. 1991). The higher penetration depth was attributed to the flow through reactor design used in the experiments that forced CO_2 through the sample using an advective rather than a diffusive gas transport process.

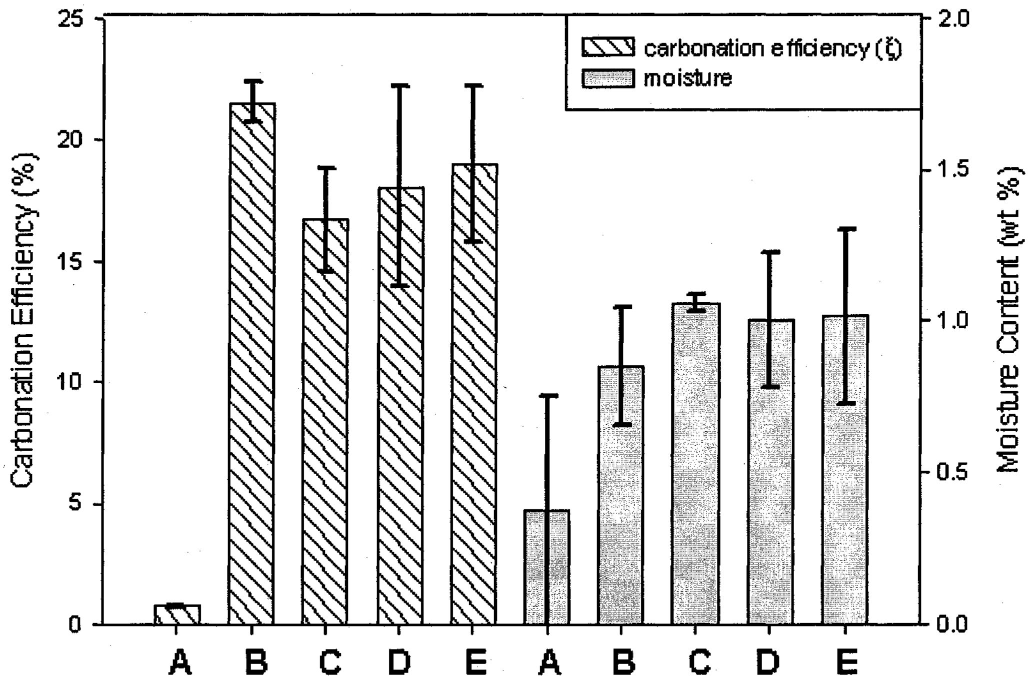

Figure 12. Spatial distribution of carbonation efficiency and moisture content in compacted grout samples. (A) non-carbonated, (B) inlet surface, (C) core, (D) outlet surface, (E) average. Error bars denote the standard deviation (σ = 1) of replicate samples.

5.4.2. Effect of the Exposed Surface Area

Loss of exposed surface area was identified as the overall limiting factor for the rate and extent concrete carbonation. Three carbonation experiments were performed to investigate the effects of increased surface area on CO_2 uptake. The premise of the experiments was that by carbonating the material as a loose substance, the overall exposed surface area would increase by eliminating the particle-particle contact causing closed, tortuous and narrow pores. In its absence only the product layer deposition upon individual particles would limit the CO_2 uptake.

In the first experiment (experiment #1), the compacted reference samples were prepared and carbonated under standard conditions for 100 minutes (Figure 13-1) in the compacted grout reactor. No surface area adjustments were made with this sample. The two other experimental results with surface area enhanced samples were compared with the reference sample.

In the second experiment (experiment #2), all preparation and carbonation conditions were kept nearly the same as experiment #1, except that the sample was not compacted (loose grout) before being carbonated at a lower CO_2 flow rate ($Q = 0.133$ Lpm) with higher moisture content ($w/c = 10$) and in the loose grout reactor (Figure 13-2). The results of experiment #2 demonstrated the effects of increasing the surface area of the grout mixture by eliminating the particle-particle contact from carbonating the sample as loose material. Water starvation was a concern in early tests with loose grout samples. Sufficient moisture is necessary in samples for the carbonation reactions to proceed. In response to the perceived water starvation, the later loose grout experiments were conducted with higher moisture content ($w/c = 10$) than the reference sample ($w/c = 0.26$).

For the third test (experiment #3), a portion of the carbonated reference grout sample from experiment #1 was dried, crushed to a fine powder and then recarbonated under standard conditions, except with a lower flow rate ($Q = 0.133$ Lpm) with higher moisture content ($w/c = 10$) in the loose grout reactor (Figure 13-3). The purpose of the experiment was to demonstrate that a previously carbonated sample showing depleted CO_2 uptake potential is capable of renewed uptake by increasing its exposed particle surface area.

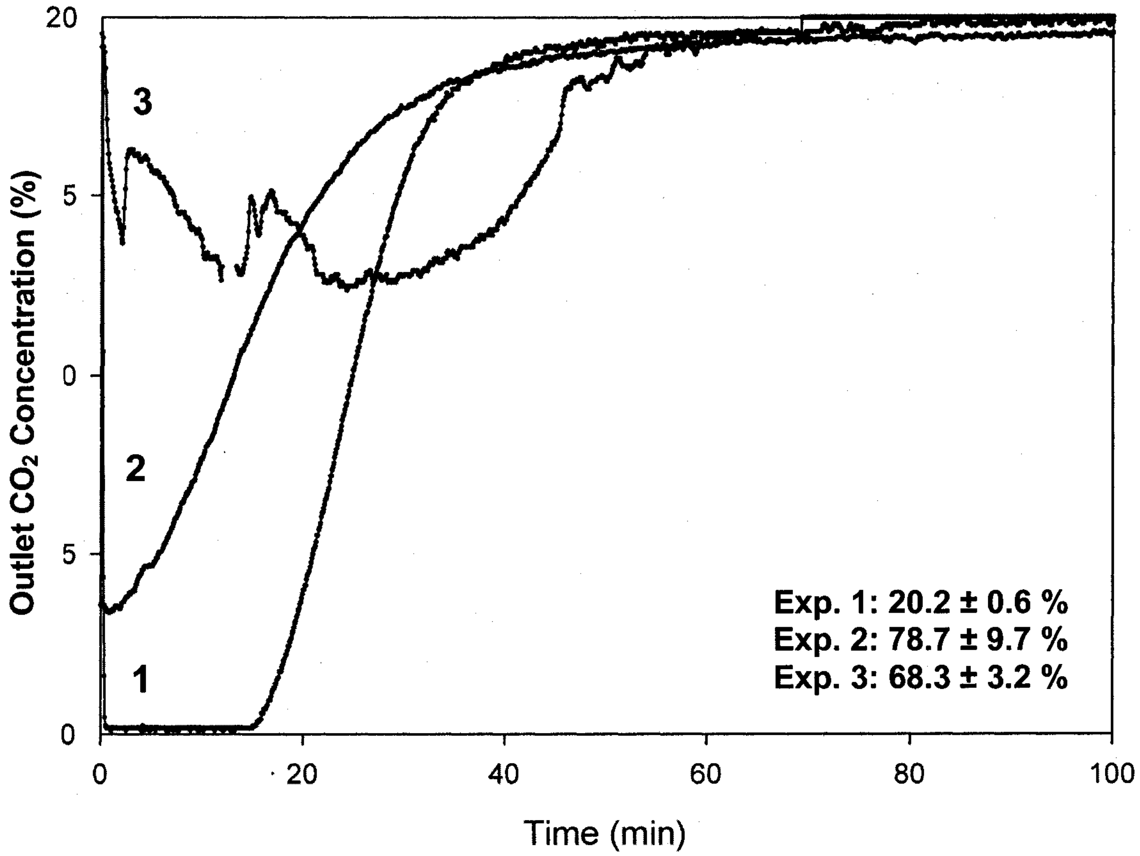

Figure 13. Carbonation plots of compacted and loose grout. (1) reference compacted grout sample, (2) loose grout sample, (3) re-carbonated loose grout sample. Error bars denote the standard deviation ($\sigma = 1$) of replicate samples.

As expected, CO_2 uptake was negligible after the reference sample (experiment #1) was carbonated beyond the commencement stage II (Figure 13-1). The final carbonation efficiency (ξ) of the control group was 20.2 ± 0.6%. Nearly full carbonation efficiency was reached within 40 min ($\xi = 78.7 \pm 9.7\%$) for the non-compacted (loose) grout sample carbonation in experiment #2 (Figure 13-2). Expressed in different units, the CO_2 mass gain of the compacted sample in experiment #2 was 39.0 wt % of cement or 290% higher than the reference sample carbonation efficiency. The results conclude that there was a very significant rise in carbonation efficiency from increasing the cement particle surface area. As seen in experiment #3 (Figure 13-3), recarbonating the reference grout sample from experiment #1 created a significant renewal in CO_2 uptake capacity ($\xi = 68.3 \pm 3.2\%$) by increasing the particle surface area. Furthermore, its uptake dynamics were far more irregular than the usual smooth carbonation profile as seen in Figures 13-1 and 7. The irregularity was explained by the presence of a heterogeneous mixture of carbonated, aged and non-carbonated material within the reference sample. Once the material was crushed and exposed the mixed material types carbonated at different rates.

The results of the surface area experiments indicated that significantly higher carbonation efficiency can be achieved by increasing the exposed surface area of cement particles within the concrete samples. Although the loose material achieved much higher CO_2 uptake, it would not yield any commercial value as a construction material. Adjustments to the CO_2 accelerated concrete curing process that increase the surface area of cement particles for enhanced carbonation efficiency, such as modifications to the aggregates, compaction pressure and the carbonation process, may provide increased carbonation.

5.5. Microstructural Assessment

Calcite was identified as the dominant carbonation product formed during the accelerated carbonation process. There are three main $CaCO_3$ polymorphs: calcite, aragonite and vaterite. Vaterite and aragonite are kinetically favoured under certain conditions; however, calcite is the thermodynamically favourable polymorph (Morse and Mackenzie 1990). The preferred product is calcite due to high thermodynamic stability and density. Backscatter Scanning Electron (SEM) and semi quantitative powder X-Ray

Diffraction (XRD) microscopy methods were employed to characterize the mineralogy of the carbonated products.

The early powder XRD analysis was performed on a grout sample carbonated under standard conditions. However, grout contains a very high proportion of silica from the fine aggregate sand. The silica peaks in the XRD results masked most of the carbonate species peaks of interest. To overcome this challenge, cement powder was carbonated under standard conditions as a loose powder. The material was analyzed by powder XRD and presumed to contain the same mineralogy as the grout sample. The diffraction pattern (Figure 14) revealed that the major constituent was calcite with traces of tricalcium magnesium silicate (Ca_3MgSiO_4) that account for the low levels of magnesium within the starting product (Table 1). Each crystalline solid has its own characteristic peak profile that is defined by the angle X-ray angle of reflection in units of 2Theta (Figure 14, X axis). The abundance of each solid is a function of the intensity of X-rays recorded at each angle of reflection shown in units of counts (Figure 14, Y axis). The insets presented in Figure 14 indicate the combined peak profile of all substances contained within the sample (top inset), and the expected peaks from calcite (middle inset) and tricalcium magnesium silicate (bottom inset) according to the 2005 ICDD diffraction pattern library. All of the significant peaks are assigned to the two major constituents. Crystalline or poorly defined structures with less than 2 wt % and 5 wt %, respectively, were below the detection limit of the instrument and could not be identified. Therefore, it may not be concluded that all of the $CaCO_3$ was in the form of calcite, and that there were no other forms of carbonate minerals present in trace quantities within the carbonated grout product.

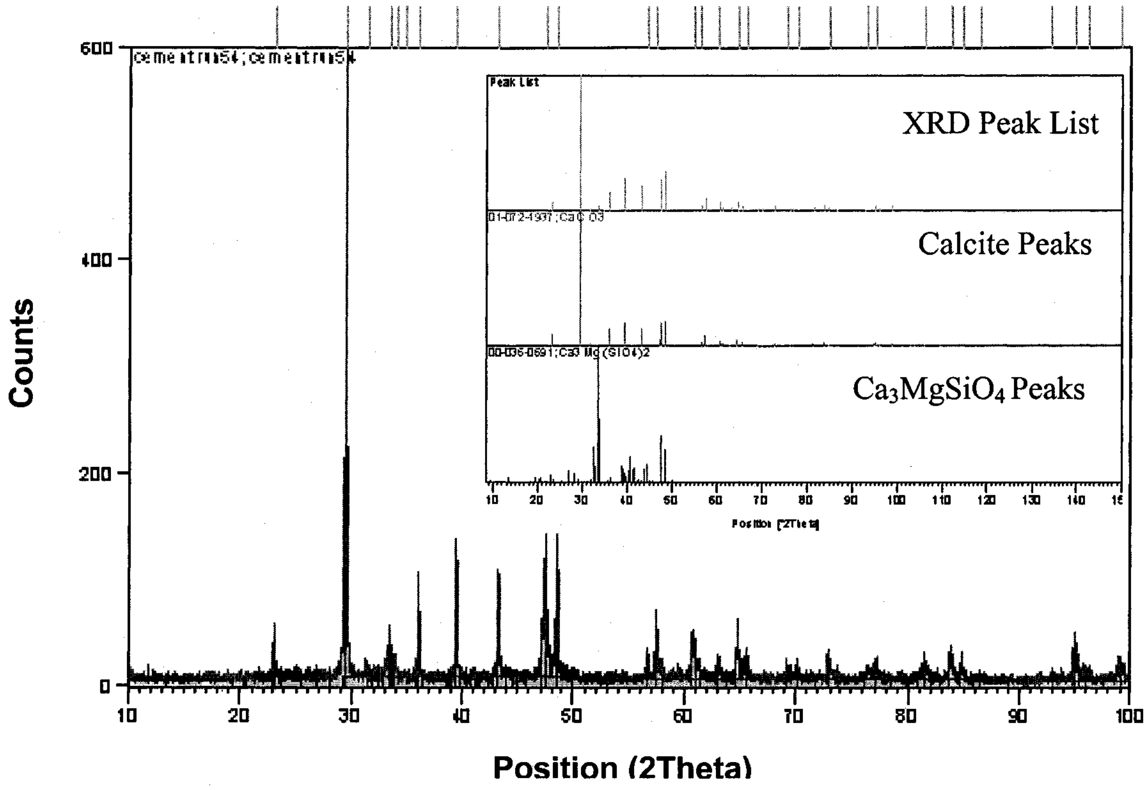

Figure 14. Powder XRD spectrum with inlaid peak list of major constituents.

SEM analysis of the carbonated material offered a qualitative view of the mineralogy. Structures in trace quantities below the detection limit of XRD can be identified with SEM microscopy if they are present in the sample. Hydrated specimens, like cement grout, must be dried by vacuum dehydration prior to SEM analysis. This step introduces a significant source of error since the drying action often causes structural damage and morphological changes of the crystal structures. Unfortunately these effects are unavoidable and but were nonetheless considered during the interpretation of the SEM results. Despite this source of error, SEM analysis of hydrated specimens remains an acceptable practice in material sciences. The SEM results corroborated the XRD findings. Calcite (Figure 15A) rhombohedral structures were predominantly observed in the images. Trace quantities of gypsum (Figure 15 Bi) and aragonite (Figure 15 Bii) were sporadically embedded in the calcium silicate framework (Figure 15 Biii).

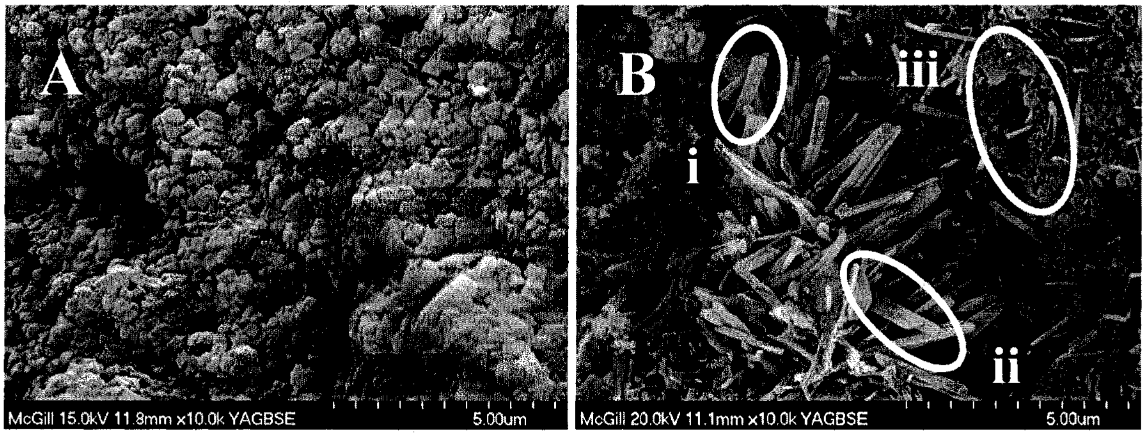

Figure 15. SEM micrograph of carbonated grout. (A) calcite, (Bi) gypsum, (Bii) aragonite, (Biii) CSH.

6. Conclusion

There are three main setbacks that have limited the adoption of CO_2 accelerated concrete curing as an industrial process and greenhouse gas mitigation method: (1) incomplete conversion, (2) shallow penetration and (3) the necessity of severe process conditions. The main objectives of the experiment were formulated to understand the causes of these issues and provide applicable solutions to resolve them. Industrial surrogates of non-reinforced concrete masonry units (CMUs) were prepared with compacted and non-compacted cement grout. The microstructural changes, dynamics and extent of CO_2 uptake of samples under mild carbonation conditions (0.1-2 Lpm, 20- 40% CO_2, 20-100% RH, 20°C, 1-3.4 atm, 30-7000min) were investigated in a bench scale flow through concrete curing reactor. The conclusions of the investigation are summarized below:

1. Calcite ($CaCO_3$) product layer coverage and associated loss of exposed particle surface area of the individual particles and pore network walls was identified as the main factor limiting the rate, depth and extent of carbonation. The product layer formation over the underlying unreacted cement material creates an impermeable barrier for Ca^{2+} and CO_3^{2-} to combine and precipitate out of solution as $CaCO_{3(s)}$. It was found that by increasing the unexposed cement particle surface area of the grout samples the carbonation efficiency may be increased nearly three fold ($\xi = 78.7$ %).
2. The carbonation dynamics are characterized by two distinct stages. Initially and very rapidly all of the CO_2 is sequestered and transformed to $CaCO_3$ as it is introduced into the reactor (stage I). Gradual product layer coverage of the unreacted material limits the ion transport and initiates the ensuing slow carbonation stage (stage II). The rate of CO_2 uptake in stage II is negligible in an industrial time scale.
3. The elemental composition of the grout feedstock was characterized by X-ray Fluorescence spectroscopy to discern the theoretical CO_2 uptake limit according to the Steinour formula (Eq. 8). The estimated CO_2 uptake potential for Type 10 St. Lawrence cement was 49.62 wt % of cement.
4. A microstructural analysis was conducted on the carbonated products using powder X-Ray diffraction (XRD) and backscatter scanning electron (SEM) microscopic methods. It was found that calcite was the major reaction product and most prevalent $CaCO_3$ polymorph. Trace amounts of Ca_3MgSiO_4 were also found in the final product.
5. SEM analysis revealed that the $CaCO_3$ product layer deposition occurred on either the individual particle surface area or within the porous network. Deposits within narrow

pores resulted in pore blockages that impeded CO_2 ingress and created localized and heterogeneous carbonate distribution within the sample.

6. A substantial process duration reduction without compromising the total CO_2 uptake was achieved by adjusting the process conditions to accelerate stage I carbonation. The rate of CO_2 uptake in stage I, prior to complete product layer coverage is directly related to the CO_2 supply rate. Increasing the CO_2 supply rate by either raising the CO_2 partial pressure of the inlet gas or preferably, raising the CO_2 gas flow rate reduced the process time by approximately 50%.
7. The grout sample hydration time (aging) prior to carbonation also limited the accelerated concrete curing process duration as well as the extent of CO_2 uptake by imposing physical limitations on ion diffusion which is analogous to the $CaCO_3$ product layer restraints. Improved process duration and CO_2 uptake were achieved by eliminating the aging period prior to carbonation. Optimal conditions were achieved when grout samples were carbonated immediately after compaction.
8. A flow through advection type reactor was designed for the project. The reactor type yielded comparable CO_2 carbonation efficiency (16.7 ± 2.1%) and full CO_2 penetration of the sample under much more moderate conditions (1 sLpm, 20% CO_2, w/c = 0.26, 40% RH, 20°C, 1 atm, 60 min) than typical accelerated concrete curing apparatus.
9. Two experimental infrared gas measurement methods were used to measure the carbonation efficiency of samples. Both methods yielded carbonation efficiency results that were comparable and not skewed by the mass gain of moisture produced within the sample. Moreover, the continuous real-time CO_2 uptake measurement method provided valuable insights into the carbonation dynamics of cement products.

10. A literature review of the global cement usage for concrete masonry units (CMUs) indicated that annually up to 550 Mt of CO_2 emissions could be permanently sequestered by the CO_2 accelerated concrete curing process, while benefiting CMU producers by improved product physical qualities and lower production time.

7. Recommendations for Future Work

Annual anthropogenic CO_2 emissions have now exceeded 20 gigatonnes and are forecasted to continue to rise over the next century (IPCC 2001). Technological innovations will play a role in combating the rising atmospheric CO_2 levels and their global warming effect. CO_2 accelerated concrete curing, a carbon capture and storage technology, has the potential to make significant CO_2 mitigation contributions. The technology is currently in the research phase; the process must be developed and tested in pilot projects before being adopted by industry on a large scale.

In the next phase of the project, the empirical data will be applied to validate a mathematical mass transport and reaction model that will aid in predicting the immediate and long term effects of mineral carbonation of porous media. Further experimental work is also being performed for a wider range of carbonation conditions including temperature, relative humidity, and moisture content as well as for different sample dimensions using the same flow through curing reactor design. Lastly, a method is under development to track the permeability changes of unsaturated grout samples during carbonation.

It is also recommended that additional research be conducted in the following topics:

1. The exposed surface area of the cement particles was found to be a critical parameter in optimizing the CO_2 uptake. The CO_2 uptake potential for CMUs is approximately 50 wt % of cement, although currently only partial carbonation can be achieved. Laboratory tests are needed to develop methods of increasing the particle surface area such as adjustments to the mix design and compaction pressure, without compromising the structural properties of the material.

2. The addition of alkaline and mineral rich waste products (blast furnace slag, steel slag) to the concrete mix design has shown potential for increasing CO_2 uptake. CO_2 uptake and material tests may be performed to investigate the added benefit using these materials in concrete.

3. The experiments were conducted with typical CO_2 partial pressures (0.2 – 0.4) of flue gases. More representative gas mixtures containing SO_2, NO_2, CO, CO_2, VOC, O_2, HCl and NH_3 may be tested in the carbonation process to define their effects on the CO_2 uptake characteristics and microstructure.

4. Material testing is essential to investigate the structural properties of samples cured with the flow through accelerated concrete curing reactor immediately after curing and after prolonged exposure to the natural environment. Properties of interest include shrinkage, durability, permeability, surface area, and porosity.

5. A wealth of knowledge can be gained from pilot projects. Research on adapting this process to an industrial scale and testing it in a pilot project will provide valuable technical and economical information.

8. References

Abanades, J. C. and D. Alvarez (2003). "Conversion limits in the reaction of CO_2 with lime." Energy and Fuels **17**(2): 308-315.

Anderson, S. and R. Newell (2004). "Prospects for carbon capture and storage technologies." Annual Review of Environment and Resources **29**: 109.

Anderson, S. and R. Newell (2004). "Prospects for carbon capture and storage technologies." Annual Review of Environment and Resources **29**: 109-142.

Bachu, S. and J. J. Adams (2003). "Sequestration of CO_2 in geological media in response to climate change: Capacity of deep saline aquifers to sequester CO_2 in solution." Energy Conversion and Management **44**(20): 3151-3175.

Bhatia, S. K. and D. D. Perlmutter (1983). "Effect of the Product Layer on the kinetics of the CO_2-lime reaction." AIChE Journal **29**(1): 79-86.

Bryant, E. (1997). Climate process and change. Cambridge, UK, Cambridge University Press.

Castro, P., M. A. Sanjuan, et al. (2000). "Carbonation of concretes in the Mexican Gulf." Building and Environment **35**(2): 145-149.

Dewaele, P. J., E. J. Reardon, et al. (1991). "Permeability and porosity changes associated with cement grout carbonation." Cement and Concrete Research **21**(4): 441-454.

DOE. (2006). "Carbon Sequestration." Retrieved May 17, 2006, from http://www.fossil.energy.gov/programs/sequestration/index.html.

DOE, U. (2006). "The FutureGen Project." Retrieved July 15, 2006, from http://www.fe.doe.gov/programs/powersystems/futuregen/.

Druckenmiller, M. L., M. M. Maroto-Valer, et al. (2006). "Investigation of carbon sequestration via induced calcite formation in natural gas well brine." Energy and Fuels **20**(1): 172-179.

Fernandez Bertos, M., S. J. R. Simons, et al. (2004). "A review of accelerated carbonation technology in the treatment of cement-based materials and sequestration of CO_2." Journal of Hazardous Materials **112**(3): 193-205.

Ferraris, C. F., V. A. Hackley, et al. (2004). "Measurement of particle size distribution in portland cement powder: Analysis of ASTM round robin studies." Cement, Concrete and Aggregates **26**(2): 71-81.

Freedman, S. (1969). "Carbonation Treatment of Concrete Masonry Units." Modern Concrete **33**(5): 33-6.

Glass, G. K., B. Reddy, et al. (2000). "Corrosion inhibition in concrete arising from its acid neutralization capacity." Corrosion Science **42**(9): 1587.

Gunter, W. D., E.H. Perkins, T.J. McCann (1993). "Aquifer Disposal of CO_2-rich gases: reaction design for added capacity." Energy Conversion and Management **34**: 941-948.

Hansen, J. (2005). Is There Still Time to Avoid "Dangerous Anthropogenic Interference" with Global Climate? A Tribute to Charles David Keeling. American Geophysical Union. San Francisco.

Hansen, J., R. Ruedy, et al. (2006). "Global Temperature Trends: 2005 Summation." Retrieved July 15, 2006, from http://www.giss.nasa.gov/research/news/20060124/.

Harrison, J. (2005). The role of concrete post Kyoto: The unrecognized sequestration solution? Dundee, Scotland, United Kingdom, Thomas Telford Services Ltd, London, E14 4JD, United Kingdom.

Hendriks, C. and K. Blok (1993). "Underground Storage of Carbon Dioxide." Energy Conversion and Management **34**: 949-957.

Herzog, H., K. Caldeira, et al. (2003). "An Issue of Permanence: Assessing the Effectiveness of Temporary Carbon Storage." Climatic Change **59**.

Holloway, S. (2001). "Storage of fossil fuel-derived carbon dioxide beneath the surface of the earth." Annual Review of Energy and the Environment **26**: 145-166.

Holt, T., J. L. Jensen, E. Lindeberg (1995). "Underground storage of CO_2 in aquifers and oil reservoirs." Energy Conversion and Management **36(6-9)**: 535-358.

Houst, Y. F. and F. H. Wittmann (2002). "Depth profiles of carbonates formed during natural carbonation." Cement and Concrete Research **32**(12): 1923-1930.

Hughes, R. W., D. Lu, et al. (2004). "Improved long-term conversion of limestone-derived sorbents for in situ capture of CO_2 in a fluidized bed combustor." Industrial and Engineering Chemistry Research **43**(18): 5529-5539.

Huijgen, W. J. J., G.-J. Witkamp, et al. (2005). "Mineral CO_2 sequestration by steel slag carbonation." Environmental Science and Technology **39**(24): 9676-9682.

IPCC (2001). Climate Change 2001: The Scientific Basis. Contribution of Working Group I to the Third Assessment Report of the Intergovernmental Panel on Climate Change. J. T. Houghton, Y. Ding, D. J. Griggset al. Cambridge, United Kingdom and New York, USA, Cambridge University Press: 881.

IPCC (2005). IPCC Special Report on Carbon Dioxide Capture and Storage. B. Working Group III of the Intergovernmental Panel on Climate Change [Metz, O. Davidson, H. C. de Coninck, M. Loos, L. A. Meyer (eds.)]. New York, Cambridge University Press: 442.

Johnson, J. W., J. J. Nitao, et al. (2001). Reactive transport modeling of geologic CO2 sequestration in saline aquifers: the influence of intra-aquifer shales and the relative effectiveness of structural, solubility, and mineral trapping during prograde and retrograde sequestration. Livermore, Lawrence Livermore National Laboratory.

Lackner, K. S., C. H. Wendt, et al. (1995). "Carbon dioxide disposal in carbonate minerals." Energy (Oxford) **20**(11): 1153-1170.

Lange, L. C., C. D. Hills, et al. (1996). "Effect of accelerated carbonation on the properties of cement-solidified waste forms." Waste Management **16**(8): 757-763.

Lange, L. C., C. D. Hills, et al. (1996). "Preliminary investigation into the effects of carbonation on cement-solidified hazardous wastes." Environmental Science and Technology **30**(1): 25-30.

Logan, C. O. (2006). Carbon Dioxide Absorption and Durability of Carbonation Cured Cement and Concrete Compacts. Department of Civil Engineering and Applied Mechanics. Montreal, McGill University. **M.Eng.:** 154.

Masters, G. M. (1997). Introduction to Environmental Engineering and Science. Upper Saddle River, NJ, Prentice-Hall.

Morse, J. W. and F. T. Mackenzie (1990). Geochemistry of sedimentary carbonates. Amsterdam, Elsevier.

O'Connor, W. K., D. C. Dahlin, et al. (2002). "Carbon dioxide sequestration by direct mineral carbonation: Process mineralogy of feed and products." Minerals and Metallurgical Processing **19**(2): 95-101.

ONS (2005). Product Sales and Trade: Concrete Products for Construction Purposes. U. O. f. N. Statistics, Her Majesty's Stationery Office.

Papadakis, V. G., C. G. Vayenas, et al. (1989). "Reaction engineering approach to the problem of concrete carbonation." AIChE Journal **35**(10): 1639-1650.

PCA. (2006). "Cement and Concrete Basics." Retrieved February 6, 2006, from http://www.cement.org/basics/concreteproducts_masonry.asp.

Rau, G. H. and K. Caldeira (1999). "Enhanced carbonate dissolution: A means of sequestering waste CO_2 as ocean bicarbonate." Energy Conversion and Management **40**(17): 1803-1813.

Reardon, E. J., B. R. James, et al. (1989). "High Pressure carbonation of cementitious grout." Cement and Concrete Research **19**(3): 385-399.

SaskPower. (2006). "Clean Coal Fact Sheet." Retrieved July 15, 2006, from http://www.saskpower.com/pdfs/clean_coal_fact_sheet.pdf.

Shideler, J. J. (1955). "Investigation of the moisture-volume stability of concrete masonry units." Portland Cement Association (D3).

Shih, S.-M., C. u.-S. Ho, et al. (1999). "Kinetics of the reaction of $Ca(OH)_2$ with CO_2 at low temperature." Industrial and Engineering Chemistry Research **38**(4): 1316-1322.

Steinour, H. H. (1959). "Some effects of carbon dioxide on mortars and concrete-discussion." J. Am. Concrete(30): 905.

Suncor. (2006). "CO_2 Sequestration." Retrieved July 21, 2006, from http://www.suncor.com/default.aspx?ID=2496.

Toennies, H. T. (1960). "Artificial carbonation of concrete masonry units." American Concrete Institute -- Journal **31**(8): 737-755.

Turkenburg, W. C. (1997). "Sustainable development, climate change and carbon dioxide removal (CDR)." Energy Conversion and Management **38**: 3-12.

UN. (1992). "United Nations Framework Convention on Climate Change." Retrieved June 3, 2006, from http://unfccc.int/resource/ccsites/senegal/conven.htm.

UN. (1998). "Kyoto Protocol to the United Nations Framework Convention on Climate Change." Retrieved June 4, 2006, from http://unfccc.int/resource/docs/convkp/kpeng.pdf.

Van Balen, K. (2005). "Carbonation reaction of lime, kinetics at ambient temperature." Cement and Concrete Research **35**(4): 647-657.

van Oss, H. G. (2006). Mineral Commodity Summaries. U. S. G. Survey.

Venhuis, M. A. and E. J. Reardon (2001). "Vacuum method for carbonation of cementitious wasteforms." Environmental Science and Technology **35**(20): 4120-4125.

White, C. M., B. R. Strazisar, et al. (2003). "Separation and capture of CO₂ from large stationary sources and sequestration in geological formations - Coalbeds and deep saline aquifers." Journal of the Air and Waste Management Association **53**(6): 645.

Wilson, E. J., T. L. Johnson, et al. (2003). "Regulating the ultimate sink: Managing the risks of geologic CO_2 storage." Environmental Science and Technology **37**(16): 3476-3483.

Wilson, M., P. Tontiwachwuthikul, et al. (2004). "Test results from a CO_2 extraction pilot plant at boundary dam coal-fired power station." Energy **29**(9-10): 1259-1267.

Young, J. F., R. L. Berger, et al. (1974). "Accelerated Curing of Compacted Calcium Silicate Mortars on Exposure to CO_2." Journal of the American Ceramic Society **57**(9): 394-397.